CFIRE

Freight Routing for Efficient, Sustainable and Reliable Travel

CFIRE 04-12
August 2014

National Center for Freight & Infrastructure Research & Education
Department of Civil and Environmental Engineering
College of Engineering
University of Wisconsin–Madison

Authors:
Jane Lin, Ph.D., Qin Chen
University of Illinois at Chicago

Yu (Marco) Nie, Ph.D., Qianfei Li
Northwestern University

Tito Homem-de-Mello, Ph.D.
Universidad Adolfo Ibañez, Santiago, Chile

Principal Investigator:
Jane Lin, Ph.D.
Associate Professor, UIC

(This page is intentionally left blank)

Technical Report Documentation Page

1. Report No. CFIRE 04-12	2. Government Accession No.	3. Recipient's Catalog No.
4. Title and Subtitle Freight Routing for Efficient, Sustainable and Reliable Travel		5. Report Date **August 2014** 6. Performing Organization Code
7. Author/s Jane Lin, Yu (Marco) Nie, Tito Homem-de-Mello, Qianfei Li, Qin Chen		8. Performing Organization Report No.
9. Performing Organization Name and Address National Center for Freight and Infrastructure Research and Education (CFIRE) University of Wisconsin-Madison 1415 Engineering Drive, 2205 EH Madison, WI 53706		10. Work Unit No. (TRAIS) 11. Contract or Grant No. **244k646**
12. Sponsoring Organization Name and Address Research and Innovative Technology Administration U.S. Department of Transportation 1200 New Jersey Avenue, SE Washington, DC 20590		13. Type of Report and Period Covered **Final Report 9/1/2010 – 8/31/2014** 14. Sponsoring Agency Code
15. Supplementary Notes **Project completed for USDOT's RITA by CFIRE.**		

16. Abstract

The goal of this research is to develop and evaluate routing models for efficient transportation that (i) aim to reduce travel time, (ii) provide reliable paths against disruptions, and (iii) factor in the emissions resulting from a given path. Specifically, the freight vehicle routing problem in this research is investigated in three aspects. The first investigation considers risk-averse freight routing problems, in which traffic conditions are treated with uncertainty (e.g., uncertain travel time or speed) and as such truck drivers are assumed as risk-averse; that is, they always prefer the expectation of a random return to the random return itself. In this research context, a random return is the random travel time itself. The second investigation incorporates microscopic vehicle operating features in an eco-routing problem. And the third investigation attempts to fill the literature gap by investigating the more realistic sustainable vehicle routing strategies by considering the joint effect of commercial vehicle load and speed on energy consumption or pollutant emissions or both. Major findings and policy implications are discussed in detailed in the report.

17. Key Words Reliability, risk-averse, greenhouse gas emissions, stochastic dominance, MOVES, eco-routing, vehicle routing problem	18. Distribution Statement **No restrictions. This report is available through the Transportation Research Information Services of the National Transportation Library.**		
19. Security Classification (of this report) **Unclassified**	20. Security Classification (of this page) **Unclassified**	21. No. Of Pages 63	22. Price **-0-**

Form DOT F 1700.7 (8-72) **Reproduction of form and completed page is authorized.**

DISCLAIMER

This research was funded by the National Center for Freight and Infrastructure Research and Education. The contents of this report reflect the views of the authors, who are responsible for the facts and the accuracy of the information presented herein. This document is disseminated under the sponsorship of the Department of Transportation, University Transportation Centers Program, in the interest of information exchange. The U.S. Government assumes no liability for the contents or use thereof. The contents do not necessarily reflect the official views of the National Center for Freight and Infrastructure Research and Education, the University of Wisconsin, the Wisconsin Department of Transportation, or the USDOT's RITA at the time of publication.

Table of Contents

Tables

Figures

EXECUTIVE SUMMARY

Introduction

The nation's transportation systems face disruptions of various sorts. Besides disastrous events, the surface transportation networks are subject to other more frequent incidents, including crashes, disabled vehicles and ever-increasing highway construction/maintenance. Meanwhile, climate change is projected to produce more extreme weather conditions, which are to threaten the reliability of the system in an unprecedented extent. Data from Federal Highway Administration (FHWA) suggest that disruptions already account for 50-60% of congestion delay in most metropolitan areas and the percentage is even higher in smaller urban areas. Travel time reliability has become an increasing concern of the network users – particularly so for freight carriers, which may lose revenue when unexpected delays strike their supply chains and disrupt just-in-time delivery. The lack of reliability often forces them to choose between running the risk of being late or budgeting a large buffer time, of which much is usually wasted. Therefore, network users are in great need of route guidance that properly weighs in the uncertainty of travel times and inform them about the reliability of their routing decisions. Such guidance should also take into consideration the fact that drivers are usually risk-averse in the sense that, given two paths with the same average travel time, they prefer the path with less variability. On the other hand, transportation contributes roughly 28 percent of the United States' total greenhouse gas (GHG) emissions, and between 1990 and 2006 the growth in transportation GHG emissions represented almost 50% of the total growth in U.S. GHG emissions. It is therefore clear that any strategy to reduce significantly the country's GHG emissions must include mechanisms and incentives to control emissions resulting from transportation.

The goal of this research is to develop and evaluate routing models for efficient transportation that (i) aim to reduce travel time, (ii) provide reliable paths against disruptions, and (iii) factor in the emissions resulting from a given path. Specifically, the freight vehicle routing problem in this research is investigated in three aspects. The first investigation (Chapter 3) considers risk averse freight routing problems, in which traffic conditions are treated with uncertainty (e.g., uncertain travel time or speed) and as such truck drivers are assumed as risk-averse; that is, they always prefer the expectation of a random return to the random return itself. In this research context, a random return is the random travel time itself. The second investigation (Chapter 4) incorporates microscopic vehicle operating features in an eco-routing problem. And the third investigation (Chapter 5) attempts to fill the literature gap by investigating the more realistic sustainable vehicle routing strategies by considering the joint effect of commercial vehicle load and speed on energy consumption or pollutant emissions or both.

Part I: Risk Averse Freight Routing Problem

This study aims to incorporate environmental measures, especially the cost of greenhouse gas (GHG) emissions, into a reliable freight routing model. GHG emission rates are generated from

Motor Vehicle Emission Simulator (MOVES) model and approximated as a function of the average link travel speed. To model uncertainty, the link travel speed is treated as a discrete random variable with a given distribution. Freight carriers are assumed to be risk-averse, which is captured by the second order stochastic dominance (SSD) relationship. The reliable freight routing model is formulated as an integer program that can be easily tailored to a variety of modelling preferences. The study experiments with eight variants of the base model, each corresponding to a different trade-off strategy between the three objectives, namely, efficiency, reliability and emission cost. The main findings from the numerical experiments are (1) modelling emission as a constraint seems more appealing due to the difficulty of estimating monetary value of emission cost; (2) the feasible set, hence the optimal solution, depends on the type of SSD constraints (time or emission), as well as the choice of the benchmark; and (3) avoiding risks in the SSD sense could increase the total cost by up to 20% in a real network.

Part II: Eco-Routing Considering Microscopic Vehicle Operating Conditions

The eco-routing problem concerned in this study addresses the optimal route choice of eco-drivers who aim to meet an emission standard imposed by regulators, while trying to find the path with minimum total operating cost, which consists of both travel time and fuel costs. The study first develops fuel consumption and greenhouse emission estimation models that link emission rates to vehicle's physical and operational properties. Unlike most studies in the literature, the emission model developed in this study retains as many microscopic characteristics as feasible in the context of route planning. Specifically, it is able to approximate the impacts of major acceleration events associated with link changes and intersection idling, and yet does not require detailed acceleration data as inputs. The proposed eco-routing model explicitly captures delays at intersections and the emissions associated with them. Using a simple probabilistic model, the impacts of different turning movements on eco-routing are also incorporated. The proposed model is formulated as a constrained shortest path problem and solved by off-the-shelf solvers. Numerical experiments confirm that ignoring the effects of turning movements and acceleration may lead to sub-optimal routes for eco-drivers. The results also suggest that vehicle characteristics, especially weight and engine displacement, may influence eco-routing.

Part III: Eco-Routing Considering the Joint Effect of Cargo Weight and Vehicle Speed

Traditional (sustainable) VRP literature typically treats all stops equally in routing. In other words, routing is affected only by link/arc properties and node properties do not influence the link/arc properties. This treatment works reasonably well in passenger vehicle VRP, however, it does not apply to urban commercial vehicle routing when loading and unloading activities are performance at customer points (nodes). This study attempts to fill the literature gap by investigating the more realistic sustainable vehicle routing strategies by considering the joint effect of commercial vehicle load and speed on energy consumption or pollutant emissions or both. Moreover, idling energy consumption and emissions at stops (due to loading and unloading at the customer's) will also be

incorporated in the optimal routing strategies. Specifically, this study presents the preliminary investigation towards filling that gap. Using a numerical example, this study has demonstrated the noticeable (joint) effects of vehicle payload, vehicle speed, and dwell time on urban commercial vehicle $PM_{2.5}$ emissions and energy consumption. Thus vehicle payload and speed could affect the visiting order of a distribution tour if minimizing the energy consumption or emissions is the objective.

Major Findings and Policy Implications

- The risk-averse freight routing model proposed in this study explore incorporates environmental measures and reliability concerns into freight routing models. Various strategies to trade-off efficiency, reliability and sustainability in the context of freight routing are explored in this research, including sensitivity analysis and incorporating the emission cost as a constraint. A notable feature of the proposed modeling framework has to do with how it addresses uncertainty. By assuming decision makers are risk-averse, the proposed models capture their reliability concerns by introducing a second-order stochastic dominance (SSD) constraint on either random travel time or random emission on a path. These constraints narrow down the feasible set to those paths whose travel time (or emission) distribution stochastically dominates a benchmark distribution in the second order. The main findings from our numerical experiments are (1) modeling emission as a constraint seems more appealing due to the difficulty of estimating monetary value of emission cost; (2) the feasible set, hence the optimal solution, depends on constraint type (time or emission), as well as benchmark choice; and (3) avoiding risks in the SSD sense could increase the total cost by up to 20% in a real network.
- The eco-routing model incorporating microscopic vehicle operating characteristics is able to approximate the impacts of major acceleration events associated with link changes and intersection idling. Perhaps more important, it accomplishes this through an approximation scheme that obviates using detailed acceleration profile as inputs. Moreover, the proposed eco-routing model explicitly captures delays at intersections and the emissions associated with them. Using a simple probabilistic model, the impacts of different turning movements on eco-routing are also incorporated. The main findings from these experiments are summarized below:
  a) Vehicle characteristics seem to influence path choice. Thus, the eco-routing model developed in this study is of practical importance because it is able to differentiate vehicle types.
  b) Incorporating turning movements and acceleration has significant impacts on eco-routing. Conventional models that simply ignore these microscopic vehicle operating conditions may provide sub- optimal route guidance to eco-drivers.
- This research has also demonstrated the noticeable (joint) effects of vehicle payload, vehicle speed, and dwell time on urban commercial vehicle emissions and energy consumption. For example, heavier vehicles with larger initial payloads can benefit more from the sustainable routing strategies which incorporate the effect of vehicle weight, and low speeds have the

greater impact than high speeds, causing higher energy consumption and emissions. The analysis results have indicated that the vehicle payload and speed could affect the visiting order of a distribution tour if minimizing the energy consumption or emissions is the objective. Idling energy consumption/emissions at stops, although considerably low compared to on-road energy consumption/emissions, may not be ignored especially in congested urban areas where customer density is high with large drop-off/ pick-up cargo weights and other special requirements are in place at the customer's (e.g., engine on to operate the refrigerator).

1. INTRODUCTION

The nation's transportation systems face disruptions of various sorts. Besides disastrous events, the surface transportation networks are subject to other more frequent incidents, including crashes, disabled vehicles and ever-increasing highway construction/maintenance. Meanwhile, climate change is projected to produce more extreme weather conditions, which are to threaten the reliability of the system in an unprecedented extent. Data from Federal Highway Administration (FHWA) suggest that disruptions already account for 50-60% of congestion delay in most metropolitan areas and the percentage is even higher in smaller urban areas (Farradyne 2000). Travel time reliability has become an increasing concern of the network users – particularly so for freight carriers, which may lose revenue when unexpected delays strike their supply chains and disrupt just-in-time delivery. The lack of reliability often forces them to choose between running the risk of being late or budgeting a large buffer time, of which much is usually wasted. Therefore, network users are in great need of route guidance that properly weighs in the uncertainty of travel times and inform them about the reliability of their routing decisions. Such guidance should also take into consideration the fact that drivers are usually risk-averse in the sense that, given two paths with the same average travel time, they prefer the path with less variability

The discussion on improving transportation, however, cannot be restricted to simply finding reliable routes. In the current context of climate change, it is imperative that sustainability issues be taken into account. For example, transportation contributes roughly 28 percent of the United States' total greenhouse gas (GHG) emissions, and between 1990 and 2006 the growth in transportation GHG emissions represented almost 50% of the total growth in U.S. GHG emissions (Cambridge Systematics 2009). It is therefore clear that any strategy to reduce significantly the country's GHG emissions must include mechanisms and incentives to control emissions resulting from transportation. On the other hand, it is important to notice that the objective of controlling emissions conflicts with minimizing travel time, as it has been shown that high vehicular speeds lead to higher emissions (Frey et al. 2003). Well-established traffic simulation models such as MOVES (US Environmental Protection Agency 2010) can accurately estimate emissions based on average vehicle speed and power.

In summary, routing models for efficient transportation must (i) aim to reduce travel time, (ii) provide reliable paths against disruptions, and (iii) factor in the emissions resulting from a given path. The goal of the research is to develop, implement and evaluate such models. Specifically, the freight vehicle routing problem in this research is investigated in three aspects. The first investigation (Chapter 3) considers risk averse freight routing problems, in which traffic conditions are treated with uncertainty (e.g., uncertain travel time or speed) and as such truck drivers are assumed as risk-averse; that is, they always prefer the expectation of a random return to the random return itself (Nagurney 2000). In this research context, a random return is the random travel time itself. The second investigation (Chapter 4) incorporates microscopic vehicle operating features in an eco-routing problem. And the third investigation (Chapter 5) attempts to fill the literature

gap by investigating the more realistic sustainable vehicle routing strategies by considering the joint effect of commercial vehicle load and speed on energy consumption or pollutant emissions or both.

2. LITERATURE REVIEW ON SUSTAINABLE VEHICLE ROUTING

Transportation consumes over 27% of all energy, of which 98% comes from petroleum use. Transportation also contributes roughly 28% of the United States total greenhouse gas (GHG) emissions. Indeed, the freight sector, especially the trucking industry, has become a major source of greenhouse gas emissions (GHGs) within transportation. The US Environmental Protection Agency (EPA) reports that the transportation sector contributes to 28% of U.S. GHGs in 2005, of which freight trucks account for 19.1% or 385.1 Tg CO2 equivalents (Davies and Facanha 2007). Even worse, the environmental impacts of the trucking industry seem to have increased at a greater pace compared to other sectors. The GHGs from freight trucks have increased about 69% from 1990 to 2005. During the same period, the contributions of light-duty vehicles to GHGs only increased by 23% (Davies and Facanha 2007). An official White House Memorandum [1] proclaims that GHGs emissions from medium-duty and heavy-duty trucks and buses will be regulated by the federal government for the first time beginning in model year 2014. With such regulations in place, tougher carbon standards that target excessive emissions from irresponsible operation practice seem within the realm of possibility.

In urban areas in the U.S., good movements account for 24% of total transportation energy consumption, 30% of the total vehicle miles traveled (VMT) and 20-50% of total transportation emissions0. Fuel cost contributes 39% of the operating cost for the trucking industry 0. All these factors have led to increasing effort in the trucking industry to come up with innovative energy-saving (and even emission-saving) vehicle routing strategies in recent years. They have also motivated research interests in sustainable vehicle routing problems.

2.1 Incorporation of Environmental Measures in Vehicle Routing Problem

Finding optimal path for freight vehicles between an origin-destination pair in a network involves different types of operating costs. Many of these costs, such as fuel consumption and labor, are closely related to prevailing travel time in the network. Meanwhile, the cost associated with vehicle emissions is attracting more attention as the transport industry begins to embrace sustainability as a guiding principle in their day-to-day activities.

Eguia et al. (2013) provided a detailed review on sustainable vehicle routing literature, in which the objective is usually to minimize the CO_2 emissions or energy consumption, typically as a function of speed. Eguia et al. (2013) also showed that the solutions for minimizing the CO_2 emissions might be the same as that for the shortest path problem under many circumstances. Figliozzi (2010) developed a vehicle routing with time window (VRPTW) algorithm for reducing CO_2 emissions and found that the proposed algorithm might provide significant emission savings for commercial vehicles especially in congested areas where vehicle speed was very low. However,

[1] www.ens-newswire.com/ens/may2010/2010-05-21-02.html, last visited on July 5, 2012)

the emission savings were not uniform because the route characteristics (e.g., speed) and other routing constraints (e.g., time window) affected CO_2 emissions differently.

The literature clearly indicates that minimizing travel time and emissions are sometime conflicting objectives, because the rates of most emissions do not change monotonically with travel speed (Rilett and Benedek 1994, Nagurney 2000). The best fuel economy, hence the lowest GHGs emission rate, usually occurs at the speed around 55 - 60 mile per hour (mpgforspeed.com, last accessed May 2014). Consequently, it is important to properly balance time and emission costs. Unfortunately, although the drivers' wage rates may be used as a reliable surrogate for the value of time, estimating the cost of emission is far more difficult and controversial. Different studies often produce vastly different estimates, ranging from as low as 3$ per metric ton to as high as 1600 $ per metric ton (Bishins et al. 2009).

There are other factors that affect vehicle emissions and energy consumption in a goods distribution tour. Arvidsson (2013) presented a load factor paradox in the urban distribution network and showed that if the truck load enforcement (i.e., minimum load mandate) was in place in an urban area then factor restriction is in enforcement then drivers had the tendency to have the heaviest goods delivered at the last stop, which had an unintended consequence of increasing the energy consumption and emissions compared to the same route with the reversed visiting order. This is because energy consumption generally increases with the vehicle load, especially for heavier trucks. Gaines et al. (1983) found that the total energy consumed by idling trucks was more than two billion gallons per year, among which the workday idling at customer stops dominated the energy usage. Therefore, the idling energy consumption and emissions should not be neglected in sustainable vehicle routing problems (VRPs).

To the authors' best knowledge, very few VRP studies in the literature have considered the effect of vehicle load (or in many instances the same as visiting order), nor the joint effect of vehicle load and speed in VRP. Suzuki (2011) developed a VRPTW algorithm with the objective of minimizing the distance but also considering the energy consumption as a function of vehicle load both on the road links and at the customer sites. The study found that the heavier items should be unloaded first and the lighter items should be unloaded later while all at the same time minimizing the distance. By changing the visiting order the study showed that the new routing strategy produced up to 6.9% energy saving. With the objective of minimizing energy consumption, Xiao et al. (2012) added the vehicle load dependent energy consumption rate to the classical capacitated vehicle routing problem (CVRP) and solved it with the simulated annealing algorithm. They concluded that considering vehicle load in the CVRP model can reduce energy consumption by 5%.

In addition, the idea of integrating environmental measures into transportation assignment models has also gained popularity in recent years. Tzeng and Chen (1993) studied a traffic assignment model that simultaneously considers travel time, travel distance and CO emission. The CO

emission on a link is modeled as a linear function of link traffic volume. The focus is to find an optimal normalized weighting vector to minimize a weighted total of the three objectives. Rilett and Benedek (1994) considered user-equilibrium and system optimal traffic assignment models in which the objective is to minimize CO emissions, which is modeled as a nonlinear function of link speed according to TRANSYT 7-F (Penic and Upchurch 1992). They conclude that the reduction of travel time and CO emissions often conflict. A similar study was conducted by (Sugawara and Niemeier 2002), albeit their goal is to understand how much CO emissions could be reduced in an assignment model devoted to minimizing them. Sugawara and Niemeier (2002) calibrated the CO emission as a fourth-order polynomial function of travel speed, using emissions information developed by the California Air Resources Board. Yin and Lawphongpanich (1998) discussed pricing schemes that would induce network flow distribution with minimum CO emission. A bi-level bi-objective pricing design model is proposed to trade off congestion alleviation and emission reduction. Ahn and Rakha (2008) examined the impacts of route choice on energy consumption and emission rates using GPS data. Using microscopic emission estimation models, their case study demonstrates that significant improvements to energy and pollutions can be achieved when motorists utilize a slower arterial route. Chen et al. (2011) examined a traffic assignment model with environmental constraints, which are imposed based on either link or area. Their study shows that such environmental side constraints can result in different equilibrium solutions. The studies cited above mainly focus on route choice and traffic assignment. Other fields, such as operations research, also see an elevated interest in developing environment-sensitive models (Figliozzi 2010, Bektas and Laporte 2011).

2.2 Eco-Driving

Of another particular interest to this study is driving behavior that aims at reducing fuel consumption and GHG emission, broadly known as *Eco-Driving*. Most Eco-Driving programs in Europe and US estimate emission improvements on the order of 5 to 15% (Onoda 2009). A recent study based on a sample of 20 California drivers (Boriboonsomsin et al. 2010) indicates emission savings of 6% and 1% on arterial streets and freeways, respectively. Most Eco-driving tips offered by these programs focus on microscopic operational tactics, such as maintaining a steady speed close to the speed limit, executing smooth deceleration, and avoiding idling. Manzie et al. (2007) demonstrates that mitigating stop-and-go motions by anticipating downstream traffic conditions could generate up to 33% fuel savings for vehicles equipped with conventional drive trains, while much smaller improvements are found for hybrid vehicles.

An important aspect often overlooked in existing eco-driving practice is the impacts of route choice. A vehicle's average travel speed, which is a predominant factor in determining emission, is highly correlated with the prevailing speed of the road on which it is operated. Once the route is selected, the aforementioned microscopic tactics have relatively small capacity to choose operating speed in favor of eco-driving. For example, it is difficult for a vehicle stuck in severe traffic congestion to maintain a steady and eco-friendly speed, which typically ranges between 55-60

miles per hour (mph) (mpgforspeed.com). To minimize emission, therefore, it seems that eco-drivers only need to choose routes such that the average speeds on all segments are as close to the eco-friendly range as possible. Two issues complicate this seemingly simple strategy, however. First, eco-drivers may have to consider other objectives, such as travel time, in their routing decision. These additional objectives may be in conflict with emission minimization, as speed increasing beyond 60 mph is known to reduce fuel economy. This conflict between emission and other conventional routing objectives has been widely noticed and modeled, e.g., related studies in traffic assignment and route choice models (Tzeng and Chen 1993, Sugawara Rilett and Benedek 1994, Benedek and Rilett 1998, Nagurney 2000, Sugawara and Niemeier 2002, Yin and Lawphongpanich 1998, Chen et al. 2011), and related studies in operations research (Maden et al. 2009, Kara et al. 2007, Bauer et al. 2009, Bektas and Laporte 2011). The second complication has to do with the fact that the average cruise speed is not the only contributing factor to vehicle emissions. Many other operating conditions, notably acceleration and idling also play a significant role. Because idling is mostly associated with waiting at intersections, the choice of turning movements has to be taken into account. The effects of turn penalty and prohibition on route choice have been noticed both in the literature (Kirby and Potts 1969, Ziliaskopoulos and Mahmassani 1996) and in practice1. Estimating the impacts of vehicle acceleration on eco-routing is more challenging for two reasons. First, unlike speed, acceleration is not well correlated with road properties and traffic conditions. Hence, it seems difficult to estimate vehicles acceleration profile at the stage of route planning. Second, including acceleration in the model would make route decision acceleration-dependent. Yet, such a microscopic behavior as choosing acceleration is very difficult for the modelers to predict. On the other hand, acceleration seems to have significant impacts on the total emission of a route. A simulation study conducted by Ahn and Rakha (2008) shows that ignoring acceleration would reverse the rank of two alternative routes (a highway and an arterial) in terms of fuel and pollutant emissions. Yet, to the best of our knowledge, microscopic vehicle operating conditions such as acceleration and idling are rarely considered in route choice models.

3. Part I: Risk Averse Freight Routing Problem

3.1 Problem Definition and Objectives

This study aims to explore ways for properly trading off efficiency, reliability and sustainability in the context of freight routing. Specifically, efficiency deals with finding paths that minimize travel delays; reliability addresses the uncertainty in traffic conditions; and the sustainability component takes into account vehicle GHGs emissions when determining the best routes. To address uncertainty, decision makers are assumed as risk-averse; that is, they always prefer the expectation of a random return to the random return itself (Friedman and Savage 1948). Following Nie et al. (2011), we propose to capture such a behavior by introducing a second-order stochastic dominance (SSD) constraint on either random travel time or random emission on a path (Nie et al. 2011). Specifically, the constraint narrows the feasible set down to the paths whose travel time (or emission) distribution stochastically dominates a benchmark distribution in the second order (e.g., Hanoch and Levy 1969). A benchmark may be established based on a preferred path or an externally defined standard. Since the SSD constraint may be applied to either travel time or emission, another focus of the study is to compare these different modeling options.

The rest of the chapter proceeds as follows. Section 3.2 presents modeling framework including the emission-speed relationship estimated from MOVES in Section 3.2.1 and several proposed reliable freight routing formulations with environmental measures in Section 3.2.2. Results of numerical experiments are reported in Section 3.3 and Section 3.4 summarizes the study and discusses future directions.

3.2 Reliable Freight Routing Model with Emission Measures

3.2.1 Emission-Speed Relationship

For the freight routing problem concerned in this study, the predominant factor in decision making is prevailing link speeds, which determine the time that a freight truck needs to traverse a link, and accordingly, the rate of GHGs emissions as it passes through. This study adopts a macroscopic approach to estimate truck emissions. Specifically, MOVES (Motor Vehicle Emission Simulator), the EPA's latest mobile emission model, is employed to build the relationship between CO2 equivalence (CO2e) and average link speed. Our proposed method first samples comprehensive emission rates (grams per vehicle-hour) in MOVES for the given truck type at various discrete speed levels. Then, a simple regression analysis is performed to fit the functional relationship.

MOVES estimates emissions using a modal-based approach. An important feature of this approach is that vehicle activities are binned into categories according to different factors. These so-called *source bins* differentiate activities according to vehicle characteristics such as fuel type, engine type, model year, loaded weight, and engine size. On the other hand, operating mode bins differentiate the emissions accord- ing to second-by-second vehicle activities defined by *vehicle specific power* (VSP) - a measure of the power demand placed on a vehicle under various driving

modes and instantaneous speed distributions, and classified according to average speed, road type, and vehicle type. After classifying activities into different bins, MOVES assigns an emission rate for each unique combination of source and operating mode bin. Once the emission rate is assigned to each source and operating mode bin, the emission rates are aggregated to produce an overall emission rate for each source-use type. A few correction factors are also applied to the emission rates to adjust for the influence of temperature, air conditioning, and fuel effects. More detailed technical discussion of MOVES can be found in US EPA (2002).

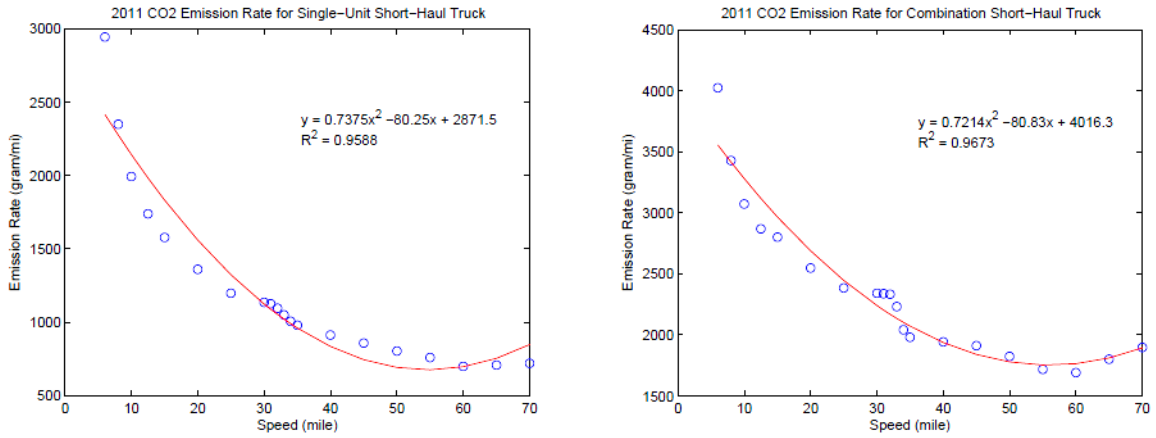

(a) 2011 CO_2 emission rates for single unit short-haul truck (b) 2011 CO_2 emission rates for combination short-haul truck

Figure 1 CO2 emission rates for two types of trucks

By running MOVES, we are able to obtain a matrix of emission rate by vehicle speed for each road type, vehicle type and analysis year. In the second step, quadratic functions are employed to fit the emission- speed relationship. Figure 1(a) and Figure 1(b) show both the original data and the fitted function for two different truck types in 2011. The plots in the figures indicate that the emission factor (gram/mile) is a non-monotone function of speed, which implies that the optimal emission is not achieved at the maximum speed. This observation confirms that one may have to balance the environmental and time-related costs to optimize the total cost. For the single unit short-haul truck, the CO2e emission rate function $r_a(\cdot)$ (gram/mile) is specified as

$$y_e(v) = 0.7335v^2 - 80.25v + 2871.5 \quad (1)$$

where v is the vehicle speed.

3.2.2 Reliable and Sustainable Freight Routing Model

The reliable freight routing problem aims to minimize the total operating cost (travel time and fuel) of travelling between a given origin-destination pair *r-s*, while taking reliability and emission costs into consideration. Let us denote l_a, v_a, t_a, h_a and e_a as the length, speed, travel time, fuel consumption and CO_2e emission on link a. Note that t_a, h_a and e_a can be computed from v_a using:

$$t_a = l_a/v_a,\ h_a = l_a y_h(v_a),\ e_a = l_a y_e(v_a) \tag{2}$$

where y_e is defined in (1) and y_h is a fuel consumption function. To estimate fuel consumption, we note that a linear relationship approximately holds between the CO2e emission and fuel consumption rates according to the carbon balance (Bath et al. 1996):

$$e_a = \gamma_1 h_a \tag{3}$$

γ_1 is near 3, as shown in (Nie and Li 2012). Hence,

$$y_h(v_a) = y_e(v_a)/\gamma_1$$

Thus, once v_a is specified, all the relevant cost components can be readily computed from (2). We shall assume that the freight carrier converts each cost component on a path to a monetary value through a general *conversion function*. Let f, g and p be the conversion function associated with travel time t_a, fuel consumption h_a and CO_2e emission e_a, respectively. For further flexibility, a weight vector is introduced so that the decision maker can adjust the objective according to specific requirements. Hence, our reliable routing problem is to

$$\textbf{P0:} \quad \underset{x}{\text{minimize}} \quad w_f f\left(\sum_{a\in A} t_a x_a\right) + w_g g\left(\sum_{a\in A} h_a x_a\right) + w_p p\left(\sum_{a\in A} e_a x_a\right) \tag{4a}$$

subject to:

$$\sum_{a\in I(i)} x_a - \sum_{a\in O(i)} x_a = d_i, \quad \forall i \in N \tag{4b}$$

$$\sum_{a\in A} c_a x_a \succeq_2 \pi_c, c = t, h \text{ or } e \tag{4c}$$

$$x_a \in \{0,1\}, \quad \forall a \in A. \tag{4d}$$

where A is the set of all links in the network. The objective function (4a) is a weighted combination of travel time, fuel and CO2 emissions; Constraint (4b) is the flow conservation constraint, where $I(i)$ and $O(i)$ are the set of incoming and outgoing arcs of node i, and d_i=-1, 1, and 0, for $i=r$, $i=s$, and $i\neq\{r, s\}$, respectively; Constraint (4d) enforces the solution variables to be integers. Finally, Constraint 4(c) incorporates reliability consideration by requiring one random path cost dominates a corresponding benchmark in the sense of second-order stochastic dominance (as the symbol $\succeq_2$ entails). This constraint requires some elaborations.

A widely adopted behavioral assumption in economics and finance (e.g., Friedman and Savage 1948) states that decision makers always choose the alternative that provides maximum expected utility. Specifically, if $\mathrm{E}[U(X)] \geq \mathrm{E}[U(Y)]$, then X is preferred to Y, where U is the utility function and $\mathrm{E}[\cdot]$ denotes the expectation operator. The following result is well known (Bawa 1975, Wu and Nie 2011)

Theorem 1. *A random variable X dominates another random variable Y in the second order, i.e, $X \succeq_2 Y$, if and only if $E[U(X)] \geq E[U(Y)]$ for any U such that $U' < 0$, $U'' < 0$.*

A decision maker is considered "risk-averse" in this study if he/she always prefers the expectation of a random variable, i.e., $\mathrm{E}[X]$, to X itself (Friedman and Savage 1948). Mathematically, this implies $\delta_X \succeq X \iff \mathrm{E}[U(\delta_X)] \geq \mathrm{E}[U(X)] \iff U(\mathrm{E}(X)) \geq \mathrm{E}[U(X)]$, where δ_X is a random variable such that $P(\delta_X = \mathrm{E}(X)) = 1$. According to Jensens' inequality, the utility function $U(\cdot)$ satisfies the above condition if and only if it is *concave*, i.e., $U'' < 0$. It follows from Theorem 1 that $X \succeq_2 Y$ if and only if all risk-averse decision makers prefer X to Y. Thus, Constraint (4c) ensures that all risk-averse decision makers prefers the random cost on the optimal path $\Sigma_{a \in A} c_a x_a$ to a benchmark π_c, which is also random. For simplicity, this study determines π_C using the corresponding cost on a predetermined benchmark path (Nie et al. 2011). However, we note that the benchmark variable may also be constructed artificially to reflect the degree of reliability requirements.

Now the question is how to represent the SSD relationship between two random variable. A widely used definition states (Hanoch and Levy 1969, Hada and Russell 1971)

Definition 1 (SSD $\succ_2$). *A random variable X dominates another random variable Y in the second order, denoted as $X \succeq_2 Y$, if $\int_t^T F_X(w)dw \geq \int_t^T F_Y(w)dw, \forall t$.*

However, using the above definition to represent SSD is neither convenient nor efficient, as it involves numerical integrations. The following result, due to Dentcheva and Ruszczynski (2003), offers a computation- ally convenient alternative.

Proposition 1. *$X \succeq_2 Y$ if and only if $E(X-\eta)_+ \leq E(Y-\eta)_+, \forall \eta \leq T$ where $0 \leq X, Y \leq T < \infty$ and $X_+ = \max(0, X)$.*

Proposition 1 can be employed to check SSD in the case of discrete distribution. Specifically,

Corollary 1. *Suppose Y has a discrete distribution with realizations y_i, $i = 1, \ldots, m$ where $a \leq y_i \leq b$, then $X \succeq_2 Y$ iff $E(X-y_i)_+ \leq E(Y-y_i)_+, i = 1, \ldots, m$.*

Using this result, Constraint (4c) can be replaced with the following

$$\sum_{a \in A} c_a(\theta) x_a - s(\theta, \eta) \leq \eta, \quad \forall \theta \in \Theta, \ \eta \in \Phi \tag{5}$$

$$\sum_{\theta} P_\theta s(\theta, \eta) \leq \sum_{\theta} P_\eta [(\pi_c(\eta) - \eta)_+], \quad \forall \eta \in \Phi \tag{6}$$

$$s(\theta, \eta) \geq 0, \quad \forall \theta \in \Theta, \ \eta \in \Phi \tag{7}$$

where $\theta \in \Theta$ is a realization of the selected random cost $c = t, h, e$ and $\eta \in \Phi$ is a realization of corresponding benchmark variable. P_θ and P_η are the probability of the realizations θ and η, respectively; $c_a(\theta)$ and $\pi_c(\eta)$ are the realized cost and benchmark cost. $s(\theta, \eta) : \Theta \times \Phi \rightarrow \mathbf{R}$ are dummy variables introduced to deal with nonlinear operator $[\cdot]_+$.

We now focus on exploring instances of the mathematical program P_0 that represent different ways of balancing the three objectives: efficiency (measured by time and fuel costs), reliability (measured by time and emissions) and sustainability (measured by emissions). Let us first consider the conversion functions f, g and p. A commonly used form is to take the expectation of the underlying path cost, and then convert it to the monetary value. Using this form, the conversion function for travel time may be formulated as

$$f_1\left(\sum_{a\in A} t_a x_a\right) = \alpha \sum_{\theta} P_\theta \sum_{a\in A} t_a(\theta) x_a = \alpha \sum_{a\in A}\left(\sum_{\theta} P_\theta t_a(\theta)\right) x_a \tag{8}$$

where α is the value of time, and may be estimated based on the truck driver's average wage rate. Similarly the conversion functions for the fuel cost and CO_2e emissions are

$$g_1\left(\sum_{a\in A} h_a x_a\right) = \delta \sum_{a\in A}\left(\sum_{\theta} P_\theta h_a(\theta)\right) x_a \tag{9}$$

$$p_1\left(\sum_{a\in A} e_a x_a\right) = \kappa \sum_{a\in A}\left(\sum_{\theta} P_\theta e_a(\theta)\right) x_a = \gamma_1 \kappa g_1\left(\sum_{a\in A} h_a x_a\right) \tag{10}$$

where δ is the average price of one unit fuel consumption and κ is the average price of one unit CO_2 emission. When the on-time delivery is important, the freight carrier may impose a penalty cost when the actual travel time deviates from a scheduled travel time τ_0. Denoting the cost of each unit time of early and late arrival as β and γ, the conversion function for travel time may be written as follows:

$$f_2\left(\sum_{a\in A} c_a x_a\right) = \sum_{\theta} P_\theta(\beta e_\theta^- + \gamma e_\theta^+) \tag{11}$$

where

$$e_\theta^- = [\tau_0 - \sum_{a\in A} c_a(\theta) x_a]_+ \tag{12}$$

$$e_\theta^+ = [\sum_{a\in A} c_a(\theta) x_a - \tau_0]_+ \tag{13}$$

As mentioned above, the freight carriers' reliability concern is captured using the SSD constraint with respect to either travel time or CO2e emissions, i.e., $c = t$ or e respectively in Constraint (4c).

For a given benchmark path, each SSD constraint effectively defines a set of feasible paths that meet the reliability requirements of risk-averse decision makers. It is worth emphasizing that the feasible set defined by the time and emission SSD constraint may be different. To see this, first note that the CO_2e emission can be viewed as a nonlinear function of travel time as in the relationship (2). Let X and Y be two discrete random variables and f be a nonlinear function. We note that $X \succeq_2 Y$ does not necessarily imply $f(X) \succeq_2 f(Y)$. To see this, we first note, according to Corollary 1,

$$X \succeq_2 Y \Leftrightarrow E[(X - y_i)_+] \leq E[(Y - y_i)+]$$

for all y_i. In the discrete case, the later equals $\Sigma_w \max[X(w) - y_i, 0]p_w \leq \Sigma_w \max[Y(w) - y_i, 0]p_w$. Let W_1 and W_2 be the sets such that $X(w) - y_i \geq 0$ for all $w \in W_1$ and $Y(w) - y_i \geq 0$ for all $w \in W_2$, respectively. Then the above inequality can be written as: $\Sigma_{w \in W_1}(X(w) - y_i)p_w \leq \Sigma_{w \in W_2}(Y(w) - y_i)p_w$. Clearly, $X(w) - y_i \geq 0$ does not necessarily imply $f(X(w)) - f(y_i) \geq 0$ when f is a nonlinear function. Hence, when the nonlinear transformation f is applied, the set W_1 and W_2 may be changed. Even if the sets remain unchanged,

$$\sum_{w \in W_1} (X(w) - y_i)p_w \leq \sum_{w \in W_2} (Y(w) - y_i)p_w \nRightarrow \sum_{w \in W_1} (f(X(w)) - f(y_i))p_w \leq \sum_{w \in W_2} f(Y(w) - f(y_i))p_w$$

Table 1 lists possible variants of P0, each corresponding to a combination of objective function and SSD constraint. In these variants, P1 is considered a base program because it neither incorporates reliability constraint nor considers environmental costs in the objective function. Compared to P1, P2 still does not consider reliability but adds the emission cost into the objective function. Yet, P2 requires estimating κ, the volatile price of CO_2e. P3 and P4 introduce time and CO_2e emission SSD constraint respectively into P 2 in order to assess the impacts of various reliability measures on the total routing cost. P5 and P6 are similar to P3 and P4 except emission cost is excluded in their objective functions. Moreover, P7 and P8 are designed to reflect the impact of benchmark path on feasible region.

Numerical experiments presented in the following section will test and compare P1 through P8 in order to understand how each of the routing objectives, as well as the way by which they are incorporated into the decision making affects the optimal routes.

Table 1 Variants of reliable freight routing models

Formulation	Objective Function	SSD Constraint
P1	$f_1 + g_1$	None
P2	$f_1 + g_1 + p_1$	None
P3	$f_1 + g_1 + p_1$	Time
P4	$f_1 + g_1 + p_1$	Emission
P5	$f_1 + g_1$	Time
P6	$f_1 + g_1$	Emission
P7	f_2	Time

P8	f_2	Emission

3.3 Numerical Experiments

Numerical experiments presented in this section consist of three parts. The first part is conducted on a small network to demonstrate the basic properties of P0. The second test compares all eight formulations over a larger network. The third example uses a real network from the Chicago region with random travel time distributions being estimated based on real traffic data. Unless otherwise specified, we set $\alpha = 20$ \$/hr, $\gamma = 40$ \$/hr, $\beta = 20$ \$/hr, $\delta = 0.0015$ \$/gram, $\kappa = 20$ \$/ton, and $\tau_0 = 0.5$ hr. δ is calculated by assuming the price of gasoline is 4\$/gallon and the gasoline weight is 6.073 lb/gallon. All models are coded in AMPL and solved by CPLEX.

3.3.1 Four-node Network

The first test network contains four nodes and five links. The random travel speed on each link can take one of the three values, 40 mph, 55 mph and 70 mph, with certain probabilities (Figure 2). Link travel times as well as fuel consumption and CO_2e emissions rates, corresponding to each speed value, can be calculated based on Equation (2). In this example, link speeds are assumed to be independently distributed.

For the given inputs, Path 2 has the least expected travel time while Path 3 has the least expected emission and fuel consumption (See Figure 2). Let ξ_k and ψ_k denote the path travel time and CO_2e emissions on path k. In terms of SSD relationship for travel time, it is easy to verify (based on Proposition 1) that (1) $\xi_2 \succeq_2 \xi_1$; (2) $\xi_3 \succeq_2 \xi_1$; (3) there is no dominance relationship between ξ_2 and ξ_3. Also, in terms of SSD relationship for emission, (1) $\psi_3 \succeq_2 \psi_1$; (2) $\psi_3 \succeq_2 \psi_2$; (3) there is no dominance relationship between ψ_1 and ψ_2.

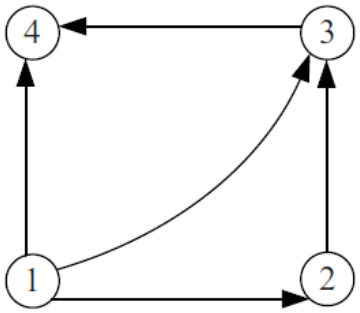

Link	Travel time (h)	Distribution
1(1-2)	0.34, 0.44, 0.6	0.3, 0.5, 0.2
2(1-3)	0.71, 0.91, 1.25	0.1, 0.1, 0.8
3(1-4)	1.07, 1.36, 1.88	0.4, 0.3, 0.3
4(2-3)	0.34, 0.44, 0.6	0.3, 0.4, 0.3
5(3-4)	0.34, 0.44, 0.6	0.2, 0.4, 0.4

Path	Sequence	Mean Time(h)	Mean Emission (gram)	Mean Fuel (gram)
1	1-4	1.4019	5936	2005.4
2	1-3-4	1.1772	6013	2031.4
3	1-2-3-4	1.2988	5546	1893.6

Figure 2 Topology, link and movement properties of the four-node network

Table 2 Optimal solutions for the four-node network

Benchmark	Path 1	Path 2	Path 3
P1	Path 2(54.86)		
P2	Path 2(56.05)		
P3	Path 2(56.05)	Path 2(56.05)	Path 3(56.33)
P4	Path 3(56.33)	Path 2(56.05)	Path 3(56.33)
P5	Path 2(54.86)	Path 2(54.86)	Path 3(55.22)
P6	Path 3(55.22)	Path 2(54.86)	Path 3(55.22)

Models P1 through P6 are solved and the results are reported in Table 2. In the table, each column corresponds to a different benchmark path. For example, column 2 represents the optimal path for each model when the benchmark is set as Path 1. In P1 and P2, no benchmark is used. Path 2 is chosen as the optimal path in both P1 and P2. Note that the difference between P1 and P2 lies in the inclusion of emission costs. However, it is clear that the impacts of emission cost are not significant ($0.71) because of the low carbon price used in the test ($20/ton). Unfortunately, it is hard to estimate the exact emission cost. To address this issue, a sensitivity analysis is conducted to examine the impact of emission cost on path choice. In our sensitivity analysis, we increase the value of emission cost until a new path is selected as optima. Path 2 remains optimal until emission cost is increased to 80$/h. After that, Path 3 is selected as the optimal path. Our sensitivity analysis implies that the value of emission cost may impact the optimal path choice. However, determination of such cost is not a easy task. Therefore, it seems more appealing to treat emission as constraint instead of objective in the face of environment consideration.

Comparing the results of P3 and P4 shows that the choice of benchmark path affects the optimal solution. In P3, when the time SSD constraint is implemented with Path 1 as the benchmark, the optimal path is Path 2. This result is expected since all three paths dominate Path 1 and Path 2 has the lowest cost. Similarly, the optimal path is Path 2 and Path 3 when the benchmark is set as Path 2 and Path 3 respectively. In these two cases, the only feasible path is the benchmark itself. Similar observations can be made for the emission constraint. When the benchmark path is Path 1, P3 and P4 admit Path 2 and Path 3 as the optimal path, respectively. Path 2 is ruled out in P4 since there is no dominance relationship between Path 1 and Path 2. Note that P4 thus generates a solution with a higher cost, which is more reliable in terms of meeting the emission standard. Comparisons between P5 and P6 generate similar insights and hence are not discussed here in detail.

3.3.2 Acyclic Network

We next test a larger acyclic network with 24 nodes and 36 links (See Figure 3(a)). We consider only one O-D pair (1-18) in the network which contains 12 paths. A joint distribution of link traversal speed with 50 realizations is created. Each realization θ is assigned a random probability

generated from a [0,1] uniform distribution such that $\sum_{\theta}^{50} {}_1 P_0 \quad 1$. For each realization θ, link speed v_i is generated as its free-flow-speed v_i^{max} times a random scalar between 0.4 and 1.

The test results are summarized in Table 3, which show that Path 4 is chosen as the optimal path in most cases. Interestingly, Path 4 dominates all other paths in terms of both time SSD constraint and emission SSD constraints. Meanwhile, Path 4 has the lowest cost in all models except for P7 and P8.

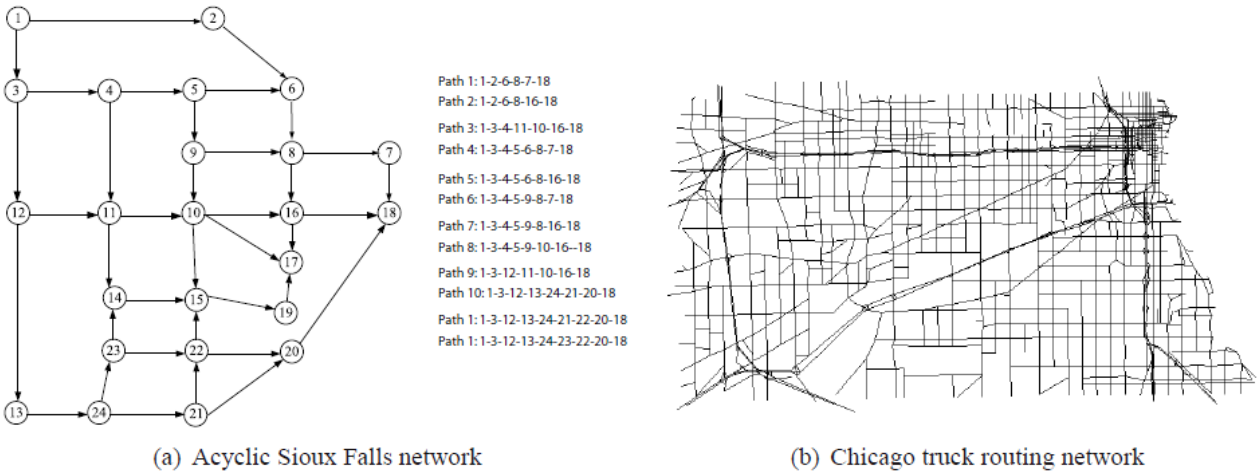

(a) Acyclic Sioux Falls network

(b) Chicago truck routing network

Figure 3 Topology of networks used in the second and third experiments

Table 3 Optimal solutions of eight models on the acyclic Sioux Falls network

Formulation	Optimal Path
P1	Path 4(7.49)
P2	Path 4(7.62)
P3	Path 4(7.62)
P4	Path 4(7.62)
P5	Path 4(7.49)
P6	Path 4(7.49)
P7	Depends on Benchmark
P8	Depends on benchmark

Table 4 Results from P7 and P8 on acyclic Sioux Falls network

Benchmark	Path 1	Path 3	Path 5	Path 6
P7	Path 5	Path 6	Path 8	Path 1
P8	Path 6	Path 3	Path 5	Path 5

For P7 and P8, Path 4 is not always the one with smallest objective value; accordingly, different paths are identified as the optima when the benchmark changes. The optimal path obtained in such a case hence reflects the change of feasible set due to the choice of the benchmark. To further examine this issue, the benchmark path is changed from Path 1 to Path 12 in this experiment. Table 4 lists the benchmark paths for which P7 and P8 generate different solutions. Since Path 2 has the least penalty cost among all paths for the given inputs, it would be the optimal path if it dominates the benchmark path. However, we found that Path 2 dominates none of the paths listed in Table 4. When Path 1 is set as the benchmark, both Path 5 and Path 6 dominate it in terms of the emission constraint. Since Path 6 has lower penalty cost, it becomes the optimal solution. However, as Path 6 is dominated by the benchmark in the case of time constraint, it is excluded from the feasible region; accordingly, the optimal path becomes Path 5. A close look reveals that, for the time SSD constraint, Path 5 ≻₂ Path 1 ≻₂ Path 6; and for emission SSD constraint, Path 5 ≻₂ Path 6 ≻₂ Path 1. This clearly indicates that the rank of stochastic dominance is changed after nonlinear transformation.

3.3.3 Chicago Network

Note that SSD constraints introduced in order to ensure that the optimal paths satisfies certain reliability standard, either in terms of travel time or emissions. In effect, incorporating these SSD constraints provides travelers protection against risk. However, because the feasible region is reduced after imposing these additional constraints, the objective function value may increase. The questions is whether the benefits of risk-aversion outweighs the extra cost. Our example is implemented to provide some insights on this question using a real-world network. To this end, we define *risk premium* as the difference in the objective function value between the model with and without SSD constraint. Thus, risk premium measures how much one has to pay in order to hedge against risk in the SSD sense. Clearly, the risk premium may be defined with respect to either the time or emission constraint.

Models P2 through P4 are considered in this experiment because they have the same objective function but different constraint structure: P2 has no constraint while P3 and P4 have time and emission SSD constraints, respectively.

The experiment is implemented on a real-world road network, which is part of the Chicago regional network (see Figure 3(b)). The upper right dense corner is the Chicago Loop. This network contains 1736 nodes and 4622 links. Travel times on links are collected from detectors on the road. These data are used to form a marginal travel time distribution for each link. We then use these marginal distributions to draw a sample that contains 100 realizations. Each realization contains travel times for all links in the network. In total, there are 100*100+100+100*100 = 20100 constraints associated with the linearization of the SSD constraint. Because of its size, solving the constrained model is time-consuming. On the computer used in the test (Intel Core i5-2400 CPU @3.1GHz, 16GB RAM, 64-bit OS), solving each constrained model takes roughly 1.5 hours.

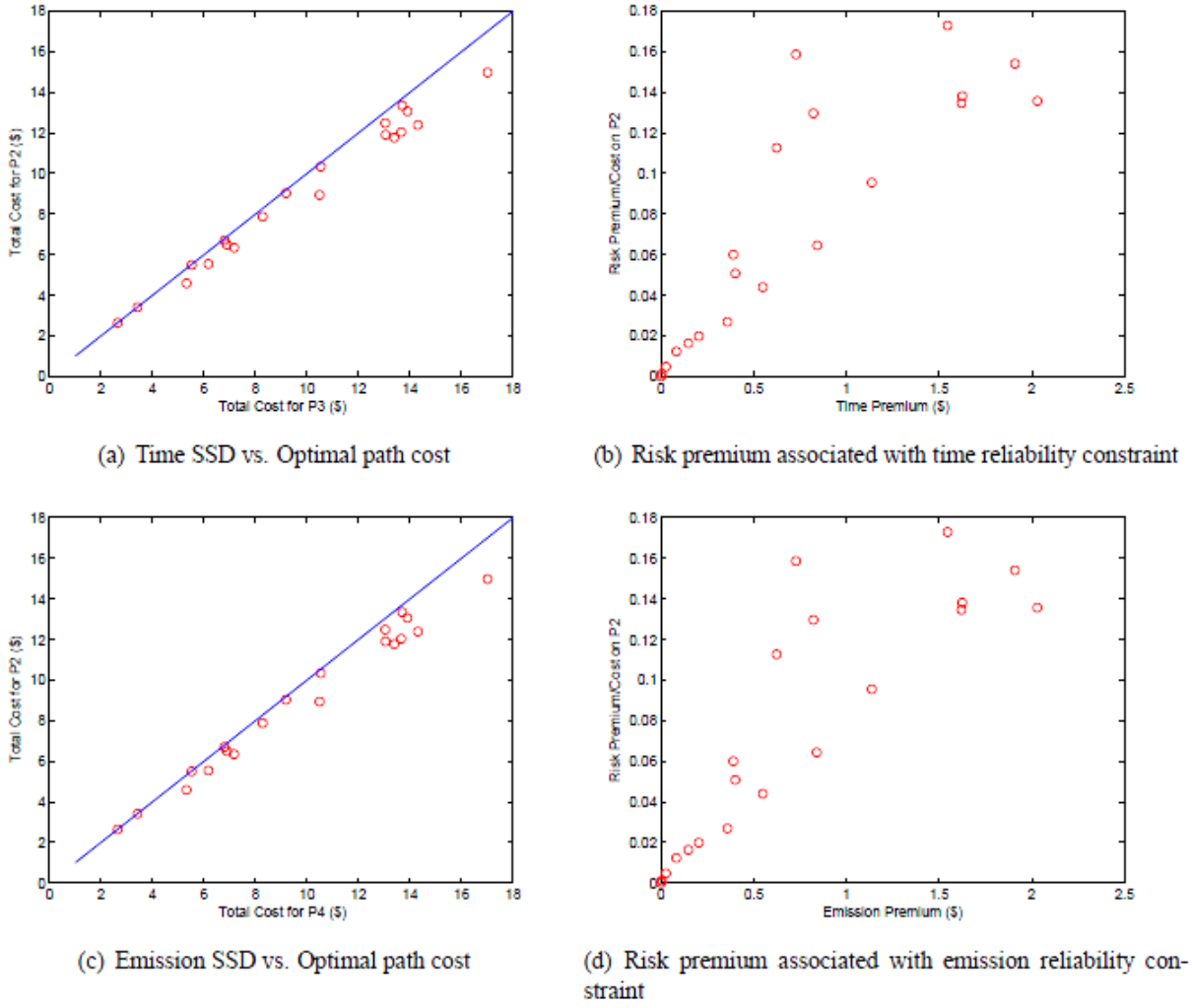

(a) Time SSD vs. Optimal path cost

(b) Risk premium associated with time reliability constraint

(c) Emission SSD vs. Optimal path cost

(d) Risk premium associated with emission reliability constraint

Figure 4 Illustration of risk premium in the Chicago network

We randomly select 20 O-D pairs and solve each of the three models for each O-D pair. Figure 4(a) and Figure 4(c) compare the objective function values in different models. In these plots, the horizontal axis is the objective function value in the SSD-constrained case, while the vertical axis is the objective value in the non-SSD-constrained case. A point in the plot represents an O-D pair. We can observe that all points lie on or below the 45 degree line, which verifies that the SSD constraint may change the solution by excluding the optimal path in the unconstrained model from the feasible set. Figure 4(b) and Figure 4(d) report the risk premium, as well as the ratio of risk premium to the optimal cost in P2. The plots indicate that in the worse case the risk premium is about 18% of the optimal cost for P2, for both time and emission cases. That is, incorporating reliability requirements could increase the total cost by up to 18%. Risk premium clearly depends on O-D pairs. For some O-D pairs, the risk premium is zero, in which case the optimal path is the same for all three models.

3.4 Conclusions

The focus of this study is to explore different modeling approaches to incorporating environmental measures and reliability concerns into freight routing models. Using MOVES, we estimate a relationship between the CO2e emission rates and link speeds. The emission rate function obtained in this study is clearly non-monotone (with respect to speed), which confirms that minimizing travel time and emissions are conflicting objectives. To trade off time and emission costs, one can simply convert both into monetary values using an estimated "market price". The main problem with this simple method is that the price of CO2 is notoriously difficult to estimate. Various solutions are explored in this research to overcome this problem, including sensitivity analysis and incorporating the emission cost as a constraint. A notable feature of the proposed modeling framework has to do with how it addresses uncertainty. By assuming decision makers are risk-averse, the proposed models capture their reliability concerns by introducing a second-order stochastic dominance (SSD) constraint on either random travel time or random emission on a path. These constraints narrow down the feasible set to those paths whose travel time (or emission) distribution stochastically dominates a benchmark distribution in the second order.

The reliable freight routing model proposed in this study has a flexible structure that can be easily tailored to a variety of modeling preferences. Taking the advantage of this flexibility, the study experiments with different strategies to trade-off efficiency, reliability and sustainability in the context of freight routing. The main findings from our numerical experiments are (1) modeling emission as a constraint seems more appealing due to the difficulty of estimating monetary value of emission cost; (2) the feasible set, hence the optimal solution, depends on constraint type (time or emission), as well as benchmark choice; and (3) avoiding risks in the SSD sense could increase the total cost by up to 20% in a real network.

The reliable routing model proposed in this study may be extended to simultaneously include time and emission SSD constraints. Clearly, such a model would have even smaller feasible sets and higher risk premiums. Because it significantly affects the feasible set and optimal solution, the benchmark choice is worth of further investigation. Indeed, such a choice may not be tied to a physical path. In the case where the emission standard is given in the form of a distribution, for example, the SSD constraint can be used to guarantee that the standard is met in the SSD sense. Developing specialized algorithms to solve the proposed models is another possible direction for future research.

4. Part II: Eco-Routing Considering Microscopic Vehicle Operating Conditions

The eco-routing model proposed in this chapter assumes that eco-drivers aim to meet an emission standard imposed by regulators, while trying to find the path with minimum total operating cost, which consists of both travel time and fuel costs. Existing CO2 emissions standards typically regulate the average CO2 emissions per unit driving distance for new vehicles. For example, the United States Environment Protection Agency (EPA) is finalizing regulations that will require the CO2 emissions of new passenger cars (light-duty trucks) be reduced from 268 (346) gram per mile (gpm) in 2012 to 225 (298) gpm in 2016, which corresponds to an increase of fuel economy from 33.6 (25.7) mile per gallon (mpg) to 39.5 (29.8) mpg. Europe Union's emission reduction target is much more aggressive, requiring all light-duty vehicles introduced after 2012 to emit 120 gram per kilometre (193 gpm) or less. Therefore, for eco-drivers, the most straightforward constraint is to require the average unit distance CO2 emissions not to exceed the published standard over all feasible paths.

Our first objective is to approximate the impacts of major acceleration events associated with link changes and intersection idling, and yet does not require detailed acceleration data as inputs. Built on the Comprehensive Modal Emissions Model (CMEM) (Barth et al. 1996, 2000), the emission model employed in this study attempts to link emission rates to vehicle's physical and operational properties (weight, drag coefficient, air conditioning etc.). However, it obviates CMEM's requirements for real-time operational parameters such as engine's gear reduction ratio and acceleration rate, which are rarely available in the context of route planning. Moreover, drivers are assumed to always drive at the prevailing speed on a road, and only accelerate/decelerate when (1) the prevailing speed changes as they move from one road to another, or (2) when they incur waiting at an intersection. A simple physical model based on the constant acceleration assumption is used to analyze acceleration induced emissions in these events. Importantly, our analyses indicate that for typical range of parameters, the majority of these "extra" emissions can be captured using a term independent of acceleration.

Our second objective is to explicitly capture idling events at intersections. Not only does the time spent in an idling event directly contribute to emissions, such an event also necessitates acceleration to the prevailing speed on the next link. Clearly, the waiting time spent at an intersection is a random variable conditional on the movement. Left turns, for instance, are likely to subject to higher waiting times compared to other movements. To this end, a probabilistic distribution is introduced to describe the waiting time associated with each turning movement. Accordingly, the expected delays and emissions associated with a given route will be evaluated based on these distributions, and used in routing decisions.

The rest of the section proceeds as follows. Section 4.1 describes the fuel and CO2 emission estimation models employed in this study. Section 4.2 analyses the impacts of accelerations on emission estimations. The eco-routing model is presented in Section 4.3, which considers the

impacts of acceleration and intersection idling on fuel and CO2 emissions. Numerical experiments are reported in Section 4.4 and Section 4.5 concludes the study and discusses directions for future research.

4.1 Fuel and CO2 Emission Model

This section briefly describes our approach to estimating fuel and CO2 emissions, which is built on CMEM (Barth et al. 1996, 2000). CMEM is preferred in this study because it provides an analytical link between an individual vehicle's characteristics (mass, speed, acceleration etc) to second-by-second fuel consumption rates. This analytical mapping does contain parameters that can be calibrated from driving cycle data.

In our model, the total engine power P is estimated as a function of vehicle speed v and acceleration a.

$$P = \begin{cases} \sum_{i=0}^{3} \alpha_i v^i + \beta a v & v \neq 0 \\ K_I V N_I + \alpha_0 & v = 0 \text{(i.e. idling)} \end{cases} \tag{14}$$

where the coefficients are specified as follows:

$$\alpha_0 = \frac{P_a}{\eta};\ \alpha_1 = Mg\frac{G + c_1}{\eta\epsilon} + c_4 K_0 V\theta(\underline{r} + c_3 v_h^2);\ \alpha_2 = Mg\frac{c_1}{c_2\eta\epsilon} - 2c_3 c_4 K_0 V v_h\theta$$
$$\alpha_3 = \frac{\rho C_d A}{2\eta\epsilon} + c_3 c_4 K_0 V\theta;\ \beta = \frac{M(1 + e_0)}{\eta\epsilon} \tag{15}$$

The above model differs from CMEM in the non-idling case in that the engine power used to overcome frictions is estimated by assuming a simple relationship between the engine reduction ratio and vehicle speed. The reader is referred to Nie and Li (2012) for more details. Once the engine power is determined, the fuel consumption rate can be estimated using

$$f = \varphi P/\lambda; \tag{16}$$

Table 5 offers detailed description of all the variables, including default values and ranges. Once the fuel rate is determined, the CO2 emission rate, denoted as $eCO2$, can be estimated based on the carbon balance (Nam 2003, Barth et al. 2000):

$$e_{CO2} = \gamma_1 f + \gamma_0 \tag{17}$$

where

$$\gamma_0 = -\frac{A_r(CO2)c_8}{A_r C + \mu};\ \gamma_1 = A_r(CO2)\left(\frac{1 - c_7}{A_r(C) + \mu} - \frac{c_5(1 - \phi^{-1}) + c_6}{A_r(CO)}\right) \tag{18}$$

Details of the parameters used in Equation (4) can be found in Table 6. We note that these estimates are aggregated over a fleet of vehicles and hence may not precisely predict emissions

for a particular car. Nevertheless, as long as the trends are reasonably captured, such inaccuracy should not adversely impact route choice. Moreover, a model with the above structure can be easily updated with newly calibrated parameters.

Equations (19) and (20) estimate the fuel and CO_2 emissions in the unit of gram per second. It is often more convenient to measure these emissions on the basis of distance. Let F and E_{CO2} denote the fuel and CO_2 emissions in the unit of gram per meter. F and E_{CO2} can be calculated as

$$F(v,a) = f/v = \frac{\phi}{\lambda}\left(\sum_{i=0}^{3}\alpha_i v^{i-1} + \beta a\right) \tag{19}$$

$$E_{CO2}(v,a) = e_{CO2}/v = \gamma_1 F(a,v) + \frac{\gamma_0}{v} \tag{20}$$

For the default valued reported in Table 6, $\gamma_0 \sim -0.016$ and $\gamma_1 \sim 3$. Hence, in practice, ignoring γ_0 from CO_2 estimation is an acceptable approximation.

Figure 5 depicts how fuel and CO2 emissions vary with the cruise speed, when acceleration is assumed to be zero (for convenience, the units have been converted from metric to the U.S. customary). A few remarks are in order here. First, the fuel emissions associated with the tractive power (F_t) in Figure 5(a) always increases with v, whereas the contribution by engine friction (F_w) always decreases with v. The tradeoff between the two seems to be the driving force behind the U-shape of the overall fuel economy curve. Second, for the default values, our model predicts that the fuel economy peaks at about 30.57 mile per gallon (assume 1 gallon of gasoline weighs 2.7896 kg) when the cruise speed is 53.2 mpg. We note that the predicted optimal speed lies in the fuel-economy maximizing range recommended by most web sites that promote eco-driving (see e.g. http://www.fueleconomy.gov/feg/driveHabits.shtml, last visited on 5/25/2012). Finally, our model predicts the lower bound of the CO2 emission is around 270 g/mile, which is very close to the aforementioned EPA's proposed CO2 emission standard for the 2012 fleet (268 g/mile). To summarize, the trend of the fuel and CO2 emissions captured by the proposed model seems to reasonably agree with the known empirical evidence.

Table 5 Description of parameters used in calculating fuel emission rates

Name	Description	Unit	Default value	Estimated range	Sources
		Constant parameters			
g	acceleration of gravity	$N.m/s^2$	9.81		(13)
c_1	constant	-	0.01		(13)
c_2	constant	m/s	44.73		(13)
c_3	constant	$rev.s/m^2$	0.0065		(17)
c_4	constant	-	1.2		(17)
η	Engine efficiency	-	0.4		(3)
		Location specific parameters			
ρ [1]	air density	kg/m^3	1.247		Wikipeida
		Vehicle specific parameters			
A [2]	frontal area	m^2	2		Internet
C_d [2]	drag coefficient	-	0.3		(13)
K_0	constant	$J/rev/liter$	200		(3)
K_I	constant	$J/rev/liter$	300		(3)
N_I	engine speed	rev/s	16.67		
V	engine displacement	liter	2.0		Internet
j	drive axle slippage	-	0.04	$0.02 - 0.05$	(13)
d	wheel diameter	m	0.4064		Internet
$\bar{r}$	constant	-	10		(17)
$\underline{r}$	constant	-	2		(17)
v_h	constant	m/s	35		(17)
		Fuel specific parameters			
λ [3]	$J/gram$	44000		(3)	
		Operation specific parameters			
G	grade	-	0		
ϵ	drivetrain efficiency	-	0.85	0.7 -0.93	(3)
ϕ [4]	fuel-air ratio	-	1.0 (1.5)	0.75 - 1.8	(3), Internet
P_a [5]	axillary power	W	1000		(16)
M [6]	weight	kg	1500		Internet
		Variables			
v	m/s	-			
a	m/s^2	-			

Notes:

1. The air density is specific to the Chicago area.
2. Default values for *A* and *Cd* are selected from various sources. They closely resemble those of a typical passenger Sedan such as Honda Accord built in 1990's.
3. The default value is based on gasoline.
4. The default fuel air ratio is 1.5 for acceleration and 1.0 for all other operating conditions.
5. The default value represents the basic accessory power. The power required to run air conditioning ranges between 1000 to 3000 *W* (9).
6. The default value is close to the curb weight of an average passenger car.

Table 6 Description of parameters used in calculating CO2 emissions

Name	Unit	Value	Comment
$A_r(CO2)$	-	44	
$A_r(C)$	-	12	
$A_r(CO)$	-	28	
μ	-	1.85	For typical gasoline only
c_5	-	0.4074	Nam (Table 5 16)
c_6	-	0.1174	Nam (Table 5 16)
c_7	-	0.01	Nam (Table 5 16)
c_8	g/s	0.0049	Nam (Table 5 16)

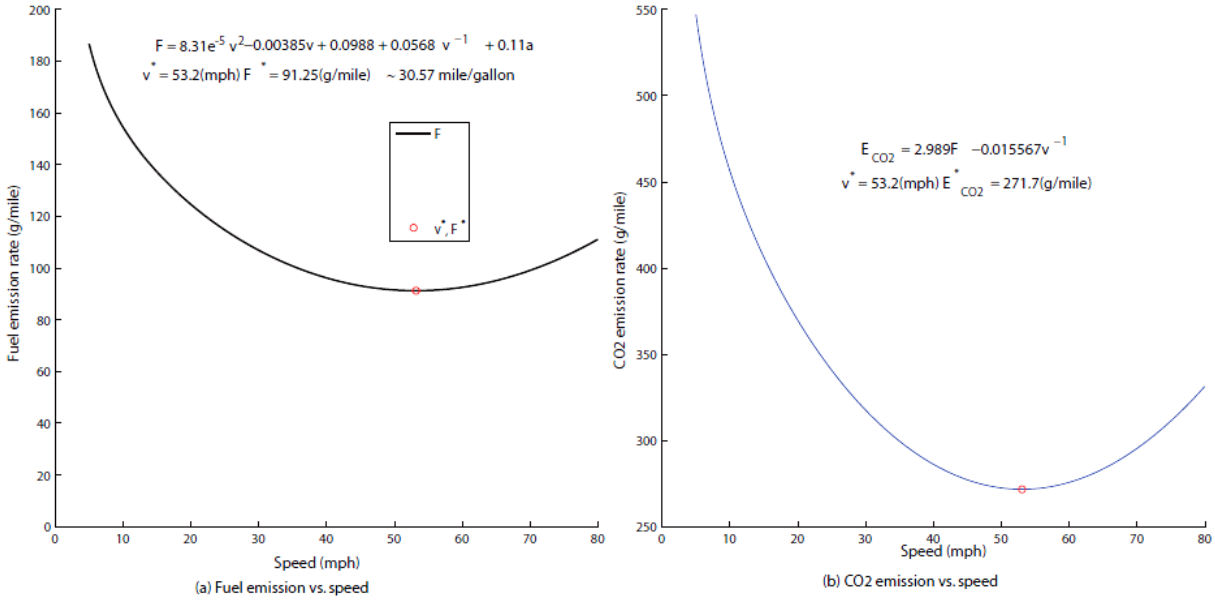

Figure 5 Fuel and CO2 emissions vs. cruise speed (a = 0). Parameters take defaults values as reported in Tables 5 and 6.

4.2 Impacts of Acceleration

Impacts of vehicle acceleration on such applications as route choice and traffic assignment are often ignored in the literature. While obtaining acceleration data is difficult, incorporating them in route choice decision seems even more challenging. To address these obstacles, this section proposes a new method that aims to approximate the impacts of acceleration while excluding acceleration as a decision variable in the model.

The proposed method divides the movement of a vehicle on each link into two stages, an acceleration/deceleration stage and a cruise stage. Once a vehicle enters a link, it will change its cruise speed to the current link's prevailing cruise speed, denoted as v_1. Denote the initial speed at the entrance as v_0, which may be either zero (if the vehicle starts the trip at the link) or the cruise speed of the predecessor link. To simplify the analysis, we assume that (1) the vehicle

enters the link at time $t = 0$; (2) the acceleration/deceleration rate a is a constant; and (3) the length of the link, denoted as l, is long enough to allow the vehicle's speed to reach v_1. As per Assumptions (1) and (2), the time and distance required to reach v_1 are respectively $t_a = (v_1 - v_0)/a$, and $l_a = 0.5(v_1^2 \quad v_0^2) \ a$. Assumption (3) implies that $l_a < l$.

Let $f(t)$ be the fuel emission rate at time t. When $v_0 < v_1$, i.e. $a > 0$, the total fuel emission on the link is computed by

$$T_F^{acc} = \frac{\phi_a}{\lambda}\int_0^{t_a} f(t)dt = \frac{\phi_a}{\lambda}\int_0^{t_a}\sum_{i=0}^{3}\left((\alpha_i(v_0+at)^i) + \beta a(v_0+at)\right)dt$$
$$= \frac{\phi_a\beta}{2\lambda}(v_1^2 - v_0^2) + \frac{\phi_a}{a\lambda}\sum_{i=0}^{3}\frac{\alpha_i v_1^{i+1}}{i+1}\left(1 - \left(\frac{v_0}{v_1}\right)^{i+1}\right)$$

where $\phi_a = 1.5$ is the fuel air ratio during acceleration. The total fuel emission for the cruise stage is given by

$$T_F^c = (l - l_a)F(v_1, 0) = lF(v_1, 0) - \frac{v_1^2 - v_0^2}{2a}\frac{\phi_0}{\lambda}\left(\sum_{i=0}^{3}\alpha_i v_1^{i-1}\right)$$
$$= lF(v_1, 0) - \frac{\phi_0}{2a\lambda}\sum_{i=0}^{3}\alpha_i v_1^{i+1}\left(1 - \left(\frac{v_0}{v_1}\right)^2\right)$$

where $\phi_0 = 1$ is the "normal" fuel air ratio. Hence, the total emission for a link of length l for acceleration is

$$T_F = lF(v_1, 0) + \phi_a\sigma_1 + \phi_a\sigma_2 + \phi_0\sigma_3 \quad (21)$$

where

$$\sigma_1 = \frac{\beta}{2\lambda}(v_1^2 - v_0^2); \quad (22)$$

$$\sigma_2 = \frac{1}{a\lambda}\sum_{i=0}^{3}\frac{\alpha_i v_1^{i+1}}{i+1}\left(1 - \left(\frac{v_0}{v_1}\right)^{i+1}\right); \ \sigma_3 = -\frac{1}{2a\lambda}\sum_{i=0}^{3}\alpha_i v_1^{i+1}\left(1 - \left(\frac{v_0}{v_1}\right)^2\right) \quad (23)$$

Clearly, the first term in Equation (21) is an estimation of total emission when completely ignoring the impacts of acceleration, and the last three terms are corrections associated with acceleration. While the total emission may be directly calculated from (21), we note that further simplification may be possible. As indicated in Figure 6(a-c), the magnitude of σ_2 and σ_3 seems of secondary significance compared to that of σ_1 for the default parameters. Specifically, Figure 6 shows that the terms associated with σ_2 and σ_3 account for less than 10% of all acceleration-related fuel emissions in most cases. While the percentage is higher for lower value of v_1, the overall emissions contributed by acceleration are small in those cases (see Figure 6(a)).

If $v_0 > v_1$, the vehicle has to decelerate from its initial speed to the current cruise speed ($a < 0$). Note that no tractive power is needed to decelerate a vehicle; instead, a is provided by the braking force. In this case, the total fuel emission becomes

$$T_F = IF(v, 0) + \phi_0(\sigma_2 + \sigma_3) \tag{24}$$

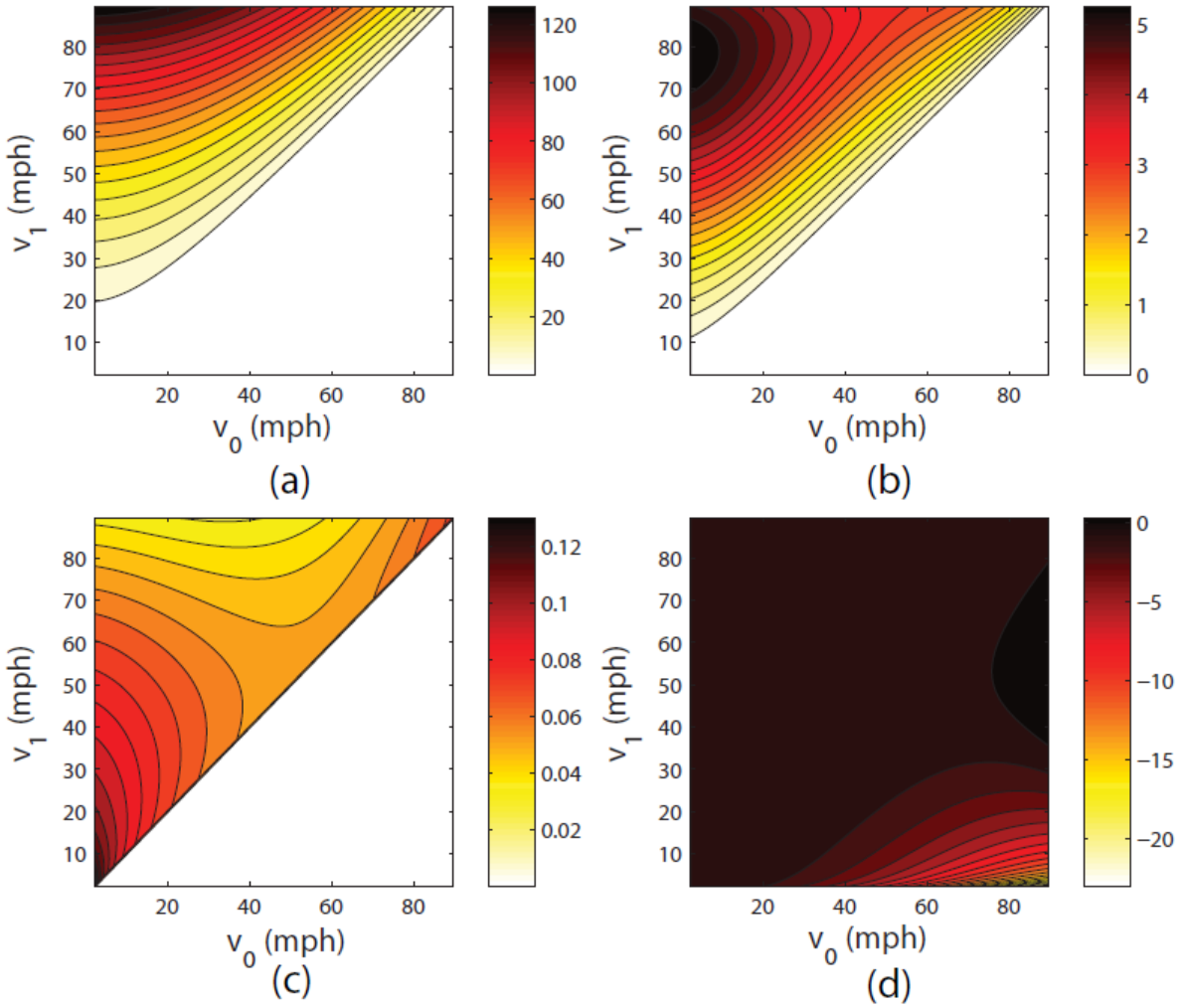

Figure 6 Impacts of acceleration on fuel emissions for different v1 and v0. Parameter values are taken from Table 1. $a = 3m/s^2$, $v0$ and $v1$ range from 1 to 40 m/s, or from 2.2 to 89.2 mph). (a) $\phi_a\sigma_1$, $(v_0 \leq v_1)$; (b) $\phi_a\sigma_2 + \phi_0\sigma_3$,$(v_0 \leq v_1)$; (c) $\frac{\phi_a\sigma_2+\phi_0\sigma_3}{\phi_a\sigma_1+\phi_a\sigma_2+\phi_0\sigma_3}$ $(v_0 \leq v_1)$; (d) $\phi_0(\sigma_2+\sigma_3)$ $(v_0>v_1)$

Figure 6(d) shows that the deceleration-related impacts $\phi_0(\sigma_2 + \sigma_3)$ may take either positive or negative values when $v_0>v_1$ - this is expected as distance-based emissions are not monotone in speed. Yet, the term is relatively small for most combinations of v_0 and v_1. It is significant only when $v_0 \gg v_1$. Even in that case the contribution of a major deceleration event barley reaches about 20 grams, an equivalent of fuel consumption in cruising about 0.25 miles at the most

favorable speed. Moreover, the impacts of different deceleration events in a route may cancel each other, because they can take positive or negative values depending on v_1.

In light of the above observations, we propose to ignore the second and third terms in Equation (21) and the second term in (24). Accordingly, the total fuel emissions of a link with cruise speed v_1 and length l are estimated as follows:

$$T_F = \begin{cases} lF(v_1, 0) + \phi_a \sigma_1 & v_0 \leq v_1 \\ lF(v_1, 0) & v_0 > v_1 \end{cases} \tag{25}$$

where σ_1 is defined in (22). Such a simplification is useful because it allows one to estimate with reasonable accuracy the impacts of acceleration on total emissions, without requiring the knowledge of actual acceleration.

Finally, we note that all plots in Figure 5 assume $|a| = 3m/s^2$. The terms associated with σ_2 and σ_3 will become larger for a smaller a because they inversely depend on a as per Equation (23). Hence, the proposed approximation will become less accurate for smaller $|a|$. Nevertheless, the reader can verify that even for an acceleration as small as $0.5m/s^2$, the fuel consumptions contributed by σ_2 and σ_3 would still be less than that of σ_1.

4.3 Eco-Routing Model

Consider a network $G(N, A)$ that consists of a set of nodes N and set of link A. Each link b is associated with a length l_b and a cruise speed v_b. Let $I(i)$ and $O(i)$ be the set of incoming and outgoing links at each node $i \in N$. Let $a \in I(i)$ and $b \in O(i)$ be a pair of links that identify a possible turning movement, denoted as m, across node i. Each m is defined by the origin link a and the destination link b. For convenience, this is written as $m^- = a, m^+ = b$. A set of all valid movements at node i is denoted as M_i. For each $m \in M_i$, $\tilde{w}_m$ denotes the waiting time of the movement, modeled as a discrete and independent random variable. Specifically, $\tilde{w}_m$ can take a discrete set of values $\{w^0, w^1, \ldots\}$ with a corresponding probability mass $\{p_m^0, p_m^1, \ldots\}$. Without loss of generality, we assume $w_m^0 = 0$ for any m. Let t_b and F_b denote the travel time and fuel emission on link b. We have

$$t_b = \frac{l_b}{v_b}; \; F_b = F(v_b, 0) l_b; \tag{26}$$

where $F(\cdot)$ are defined in Equation (19). Further, the waiting time and fuel emissions associated with the movement m, denoted as $\hat{t}_m$, $\hat{F}_m$ and $\hat{E}_m$ respectively, are given by

$$\hat{t}_m = \sum_{k=0} w_m^k p_m^k; \tag{27}$$

$$\hat{F}_m = \max(0, \frac{\phi_a \beta (v_{m^+}^2 - v_{m^-}^2)}{2\lambda} p_m^0) + \sum_{k=1} p_m^k (\frac{\phi_a \beta v_{m^+}^2}{2\lambda} + P_I \frac{\phi}{\lambda} w_m^k); \tag{28}$$

Note that $\hat{t}_m$ is simply the expected waiting time on m, whereas $\hat{F}_b$ consists of both the emission associated with engine idling (because of waiting) and the extra energy consumed to accelerate the vehicle from stationary to the cruise speed on the next link m^+ (as defined in (22)). When the waiting time is zero, the extra energy consumption is associated with the speed change from m^- to m^+, and equals zero if $v_{m^-} > v_{m^+}$. To calculate the CO2 emissions on link b and movement m, denoted as E_b and $\hat{E}_m$ respectively, we use the following approximation

$$E_b = F_b \gamma_1; \hat{E}_m = \hat{F}_m \gamma_1 \tag{29}$$

where γ_1 is defined in (18). We note that the CO_2 emissions given by (29) ignore the effects of γ_0 (cf. Equation 17), which would lead to slight overestimation of CO2 emissions. As explained before, however, such effects are expected to be quite small.

We assume that eco-drivers aim to choose a route that minimizes the total travel cost, while meeting a given CO_2 emission standard. For the convenience of representing turning movements, we assume that a trip starts on link r and ends on link s. Our eco-routing problem is formulated as follows:

$$\min \sum_{b \in \mathcal{A}} (W_t t_b + W_f F_b) x_b + \sum_{i \in \mathcal{N}} \sum_{m \in M_i} (W_t \hat{t}_m + W_f \hat{F}_m) y_m \tag{30a}$$

subject to:

$$\sum_{m \in M_i, m^- = b} y_m = x_b, \forall i \in \mathcal{N}, b \in I(i) \tag{30b}$$

$$\sum_{m \in M_i, m^+ = b} y_m = x_b + q_b, \forall i \in \mathcal{N}, b \in O(i) \tag{30c}$$

$$\sum_{b \in \mathcal{A}} E_b x_b + \sum_{i \in \mathcal{N}} \sum_{m \in M_i} (\hat{E}_m) y_m \leq \sum_{b \in \mathcal{A}} l_b x_b \bar{E} \tag{30d}$$

$$q_b = \begin{cases} 1 & b = r \\ -1 & b = s \\ 0 & \text{otherwise} \end{cases} \quad \forall b \in \mathcal{A} \tag{30e}$$

$$x_b = 0, 1; \forall b \in \mathcal{A} \tag{30f}$$

$$y_m = 0, 1; \forall m \in M_i, \forall i \in \mathcal{N}, \tag{30g}$$

In this formulation, x_b and y_m are solution variables that depict routing decisions. The objective function (30a) represents the total expected cost of a given route, where W_t and W_f are the value of travel time and the prevailing price of fuel, respectively. t_b, F_b, $\hat{t}_m$ and $\hat{F}_m$ are defined in Equations (26-28). Constraints (30b-30c) state the link-based flow conservation condition. Constraint (30d) requires that the expected emission on the path should be lower than an established standard. Constraint (30e) defines the demand between links r and s as 1. Finally, Constraints (30f -30g) require x_b and y_m be binary variables.

4.4 Numerical Experiments

In this section, two numerical experiments are conducted to test the eco-driving model proposed in the previous section. The first example is designed to examine the sensitivity of the model to selected vehicle characteristics (such as engine displacement, weight, auxiliary power). The second example aims to demonstrate the impacts of acceleration and idling on the route choice decision. Unless otherwise specified, we set $W_t = 15\$/\text{hour}$ and $W_f = 0.0015\$/\text{gram}$. Note that W_f is calculated by assuming the price of gasoline is \$4/gallon and the gasoline weight is 6.073 lb/gallon. The models are coded in AMPL and solved by CPLEX.

4.4.1 Impacts of Vehicle Characteristics

In this section, a simple 4-node network is constructed to illustrate the impacts of vehicle characteristics, as shown in Figure 7. The first number in the triplet is link number while the second and third being link length and speed respectively. Waiting time distribution of all movements, as well as t_m and F_m, is also listed in Figure 7. In the movement table, the link 0 and 6 are dummy links created for origin and destination. We assume the prevailing speed on these links is 0. Our test is conducted on four cases involving three different types of vehicles, as detailed below.

1. passenger car: $M = 1500kg$, $C_d = 0.3$, $V = 2L$, $P_a = 1000W$
2. passenger car with air condition turned on: $M = 1500kg$, $C_d = 0.3$, $V = 2L$, $P_a = 3000W$
3. minivan: $M = 2730kg$, $C_d = 0.35$, $V = 3.6L$, $P_a = 1000W$ [5]
4. light duty truck: $M = 1900kg$, $C_d = 0.53$, $V = 5L$, $P_a = 1000W$ [6]

Parameters not mentioned above take the default values reported in Table 5. Because the network contains only three paths, the emission constraint is not used to filter out paths when we solve the eco-routing model. Instead, emissions on each path are calculated separately.

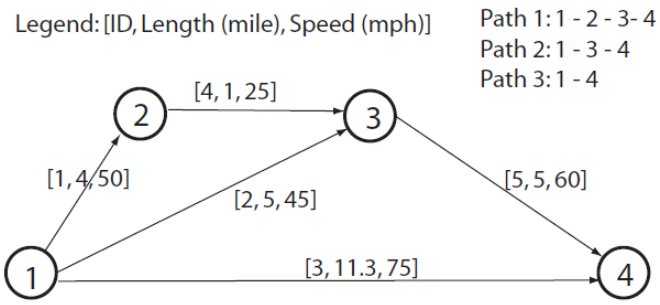

Movement	Node	From	To	$\widetilde{w}_m$ (min)	p_m	$\hat{t}_m$ (min)	$\hat{F}_m$ (gram/mile)
1	1	0	1	0	1	0	114.2
2	1	0	2	0	1	0	92.5
3	1	0	3	0	1	0	222.7
4	2	1	4	0	1	0	19
5	3	2	5	0, 2	0.5, 0.5	1	138.4
6	3	4	5	0, 1	0.5, 0.5	0.5	164
7	4	3	6	0, 1	1	0	0
8	4	5	6	0, 1	1	0	0

Figure 7 A simple four-node network

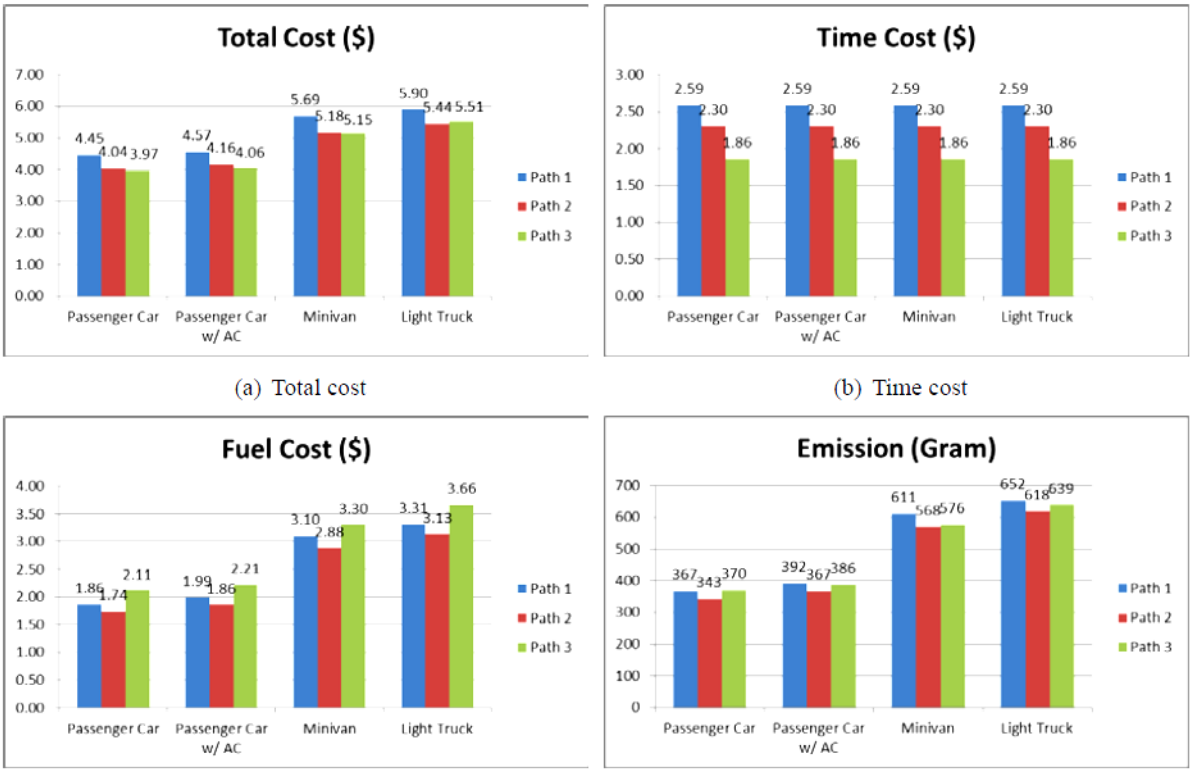

(a) Total cost (b) Time cost

(c) Fuel cost (d) Emission

Figure 8 Path cost and emissions for different vehicle types

Figure 8(a) summarizes the total cost of the 4 types of vehicles on each path. Evidently, the vehicle characteristics affect the total cost on the same path. In this case, the total costs on all

three paths increase when the vehicle type is changed from passenger car to minivan and then to light truck. However, the magnitude of the increase depends on the type. Because of that, a light truck driver would rank the three paths differently than those who drive other vehicles. Specifically, the truck driver would consider Path 2 as the optimal path when the drivers of all other vehicles would choose Path 3, which is the all expressway option. Such differences results from the high fuel cost of light truck on Path 3, see Figure 8(c). Even though Path 3 (highway) is slightly longer, its high speed leads to short travel time, which compensates high fuel cost for passenger cars and minivans. Yet, as light duty truck's large engine displacement leads to much lower fuel efficiency, the time benefit of traversing expressway cannot offset the fuel cost. Consequently, this experiment provides an example in which the path choice depends on the type of vehicle. In addition, the above results indicate that the impact of using air conditioning during operation is insignificant. Turning on air conditioning results in 25 gram (less than 3%) more CO2 emissions and about 10 cents more fuel cost in a 10-mile journey. Thus, avoid air conditioning while driving does not seem to be a worthwhile sacrifice for the sake of sustainability.

4.4.2 Impacts of Acceleration and Idling

In this section, a simple grid network that mimics a portion of a typical city center is constructed. The length of all streets is set to 0.7 miles and the speed limit is 30 mph on bold segments and 25 mph on regular segments (cf. Figure 9). The network consists twelve links and nodes A and B are set as the origin and destination for eco-routing. There are six possible paths and eighteen possible movements for the given O- D pair. The movements are grouped into three categories: left turns, right turns and through movements. Movements in the same category are assumed to have the same waiting time distribution, as reported in Figure 8. As designed, the left turns cause longest expected delay while right turns have the lowest expected delay. Finally, the emission standard $\bar{E}$ is set to 400 gram per mile to ensure the constraint is not binding.

To demonstrate the effects of acceleration and idling, the following four scenarios are considered, each corresponding to a specific objective function.

Case 1: The objective function is set as $\Sigma_{b\in A}(W_t t_b + W_f F_b)x_b + \Sigma_{i\in N}\Sigma_{m\in Mi}(W_t \hat{t}_m + W_f \hat{F}_m)y_m$, which consists of both time cost and emission cost. Time cost (fuel cost) refers to the sum of time (fuel) cost on the path and waiting time (fuel consumption) at intersections.

Case 2: The objective function is set to $\Sigma_{b\in A}(W_t t_b + W_f F_b)x_b + \Sigma_{i\in N}\Sigma_{m\in Mi} W_t \hat{t}_m y_m$, which suppresses the effect of acceleration.

Case 3: The objective function is set to $\Sigma_{b\in A}(W_t t_b + W_f F_b)x_b$. That is, the effect of turning movements is not taken into account.

Case 4: The objective function is set to $\Sigma_{b\in A} W_t t_b x_b$, which represents the conventional shortest path problem.

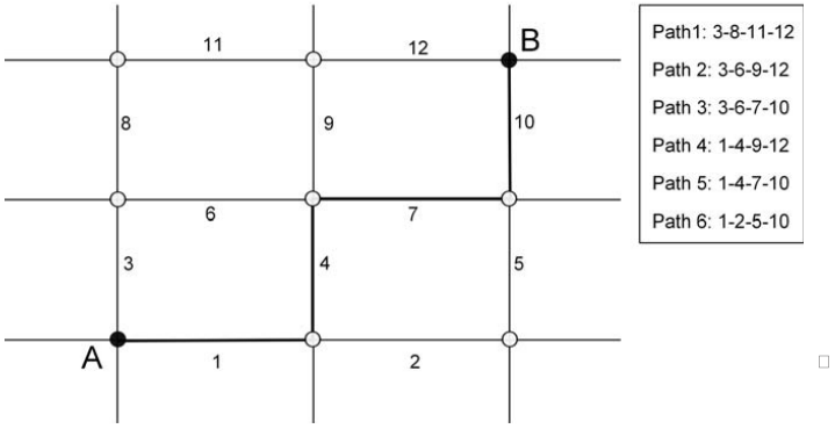

Movement	Delay (min)	Probability	Expected Delay (min)
Left	0, 1.2, 1.8	0.2, 0.3, 0.5	1.26
Through	0, 0.6, 1.2	0.5, 0.3, 0.2	0.42
Right	0, 0.6	0.5, 0.5	0.3

Figure 9 Network topology and movement properties of the grid network

The results from CPLEX indicate that the optimal path in the base case (i.e. Case 1) is Path 1. When the effect of acceleration is ignored, the optimal path becomes Path 4 or 5 (they have the same optimal cost). When turning movements are not considered, the optimal path is changed to Path 5. Thus, the consideration of microscopic vehicle operating conditions does affect eco-driving. For the purpose of verification, Table 7 enumerates all six paths and computes their total costs in each scenario.

Table 7 Total costs of all paths (All in monetary value except for 'Emission')

Path	Case 1	Time Cost [1]	Fuel Cost [2]	Emission (gpm)	Case 2	Case 3	Case 4
1	3.24	2.55	0.69	377.7	3.17	2.78	2.16
2	3.55	2.84	0.71	390.3	3.45	2.78	2.16
3	3.28	2.58	0.70	382.8	3.18	2.58	1.98
4	3.25	2.55	0.70	383.3	3.15	2.58	1.98
5	3.28	2.58	0.70	384.9	3.15	2.37	1.05
6	3.28	2.58	0.70	384.2	3.18	2.58	1.98

1. the breakdown of time cost in Case 1
2. the breakdown of fuel cost in Case 1

The effect of turning movement may be illustrated by comparing paths 1 and 2. If turning movements and acceleration are taken into consideration (Case 1), eco-drivers would prefer path 1 ($3.24) to Path 2 ($3.55). This is because Path 1 only has right turns and through movements while Path 2 include one left turn and two right turns, which renders increased time cost and fuel consumption. When the effect of turning movements is ignored, however, both paths (1 and 2) admit the same total travel cost ($2.78) -this is expected as they are exactly the same length

and free flow travel time. The extra cost on Path 2 in Case 1 clearly comes from waiting at intersections (both in terms of idling and implied acceleration events). Clearly, such a cost could potentially change the path ranking. Note that this example only shows the saving from avoiding one left turn. Savings could be much larger in a real network where multiple left turns may be included in an otherwise "good" path.

Let us now compare paths 5 and 6 to show the effect of acceleration. When acceleration is not taken into account (case 2), Path 5 ($3.15) is better than Path 6 ($3.18) in terms of total cost. Yet, when acceleration is taken into account (Case 1), the costs of the two paths are identical ($3.28). Note that Path 5 is the conventional shortest path with the minimum travel cost $1.05 (Case 4) since all links on Path 5 have the higher speed (30 mph). However, compared to Path 6, Path 5 contains two more turns, one left and one right. Clearly, the idling cost at the intersection is still not enough to offset all the benefits of staying on the high speed links. Yet, stopping at intersection also implies that the vehicle has to accelerate back to the normal speed. When these costs are accounted, Path 5 is no more attractive than Path 6.

4.5 Conclusions

The eco-routing model proposed in this study adds several new features into a growing body of environment- sensitive transportation modeling literature. Unlike most studies in the literature, the emission model developed in this study retains as many microscopic characteristics as feasible in the context of route planning. Our emission model is able to approximate the impacts of major acceleration events associated with link changes and intersection idling. Perhaps more important, it accomplishes this through an approximation scheme that obviates using detailed acceleration profile as inputs. Moreover, the proposed eco-routing model explicitly captures delays at intersections and the emissions associated with them. Using a simple probabilistic model, the impacts of different turning movements on eco-routing are also incorporated. Finally, the greenhouse emissions are introduced into the model as a constraint, inspired by EPA's regulation of new vehicle emission standards. Among other benefits, this approach bypasses the nasty task of estimating the price of CO2.

The proposed model is tested using numerical experiments designed to highlight the aforementioned features. The main findings from these experiments are summarized below:

c) Vehicle characteristics seem to influence path choice. Thus, the eco-routing model developed in this study is of practical importance because it is able to differentiate vehicle types.
d) Incorporating turning movements and acceleration has significant impacts on eco-routing. Conventional models that simply ignore these microscopic vehicle operating conditions may provide sub- optimal route guidance to eco-drivers.

Developing efficient solution algorithms for the eco-routing problem is a logical next step and an on- going effort. While the problem is known to be NP-complete, many efficient heuristics do exist that can make use of the special structure of the underlying problem. A few components in the proposed emission model requires calibration and validation, particularly the speed/gear reduction relationship, the simplifications made to engine friction calculation and important default values (e.g. fuel-air ratio under rich mix conditions). The eco-routing model discussed in this study is but a building block for higher-level transportation models (such as traffic assignment, network control, design and management) that focus on eco-driving behavior. Extending the results from this study to those models constitutes an interesting direction for further investigation.

5. Part III: Eco-Routing Considering the Joint Effect of Cargo Weight and Vehicle Speed

This research attempts to fill the literature gap by investigating the more realistic sustainable vehicle routing strategies by considering the joint effect of commercial vehicle load and speed on energy consumption (or CO_2 emissions) or pollutant emissions or both. Moreover, idling energy consumption and emissions at stops (due to loading and unloading at the customer's) will also be incorporated in the optimal routing strategies.

Specifically, this study presents the preliminary investigation towards filling that gap. Using a numerical example we will demonstrate the complexity of optimal commercial vehicle routing based on energy consumption and/or emissions many factors (e.g., link speed, vehicle load, dwell time) often times do not work in the same direction for energy consumption and/or emissions. In addition, loading/unloading cargo weight at a customer stop will affect the vehicle load and thus the energy consumption and emissions in the rest of the route, which means the visiting order of a commercial vehicle to customers matters and makes the vehicle routing problem more complicated than the traditional shortest-path based routing. And new optimization algorithms to solving such routing problems may be in order.

This chapter is organized as follows. Section 5.1 describes the problem and the study approach followed by discussions of data source and parameter estimation. Section 5.2 presents the numerical example results followed by sensitivity analyses of a set of key factors in Section 5.3. Lastly, study conclusions are provided in Section 5.4.

5.1 Study Approach and Scenario Setting

5.1.1 Problem Setting

Consider the following graph: suppose there are n customers with demand D_i ($i=1,...,n$) served by one vehicle departing and returning to the same depot 0. The customer location (coordinates) and the distance of the arc connecting from node i to node j, L_{ij}, ($i=0,..,n$, $j=0,..,n$, $i\neq j$) are known. Assume that the total customer demand does not exceed the vehicle capacity – in other words, the vehicle is able to visit all the customers in one vehicle load. There are different routing options (or visiting orders) to serve the customers depending on the selected objective (i.e. distance, energy consumption, emissions, or any combination of the three). That is, for a selected route option,

(a) Total pollutant emissions are the sum of all traveled arc emissions and node idling emissions defined as follows:

$$Emissions = \sum_{i=0}^{n} \sum_{j=0}^{n} EFL_{ij} * L_{ij} * x_{ij} + \sum_{i=1}^{n} EFN_i * DW_i \quad (31)$$

where, EFL_{ij} is the emission factor (in grams/mile) on arc ij ($i=0,..,n$, $j=0,..,n$, $i\neq j$)

L_{ij} is the length (miles) of arc ij

x_{ij}=1 if arc ij is visited , otherwise, x_{ij}=0;

EFN_i is the emission factor (grams/hr) at node i ($i=1,...,n$);
DW_i is the dwell time (hrs) at node i ($i=1,...,n$)

(b) Total energy consumption is calculated in the similar fashion to the total emissions, by substituting the emission factor (in grams/mile) with energy consumption rate (in Joules/mile).

(c) Total travel distance is the sum of all visited arc lengths (in miles):

$$distance = \sum_{i=0}^{n} \sum_{j=0}^{n} L_{ij} * x_{ij} \quad (32)$$

5.1.2 Study Approach

In this preliminary investigation, the distance-based, emission-based and energy-based routing options are compared and illustrated through a numerical example, and a number of sensitivity analyses are performed on vehicle weight (a surrogate for vehicle payload), arc average speed, cargo type and network topology to examine the effects of those factors on the routing decisions.

The numerical example is adopted from Xiao et al. (2012) with modification. In the example, there are three customers (n=3) served by a fully loaded single-unit truck departing and returning to the same depot (D). The truck has a gross vehicle weight (GVW) of 30,000 lbs, with a curb weight of 8,000 lbs. Assume that the vehicle has 20 units of payload (the unit demand is 1,100 lbs = (30000-8000)/20). The customer demand (in units) and location (coordinates) are summarized in Table 8. The arc distance is Euclidean distance, and further assume the arcs are representing urban arterials with a speed of 30mph. Dwell time at each customer stop is also showed in Table 8. Detailed explanation is provided in Section 2.3 on how dwell time is estimated at stops.

Table 8 Setup of Numeric Example

Place	ID	Coordinate	Demand(units)	Dwell time (hrs)
Depot (D)	0	(1,1)	0	0
Customer1(C1)	1	(2,3)	8	2.0
Customer2(C2)	2	(4,2)	10	2.4
Customer3(C3)	3	(10,10)	2	0.6

The U.S. Environmental Protection Agency's Motor Vehicle Emission Simulator (MOVES) is used to estimate the emission factors – $PM_{2.5}$ is chosen to be the pollutant in this investigation – as well as energy consumption rate as a function of both speed and vehicle weight (US EPA 2010). There are two sets of $PM_{2.5}$ emission factors:

- Arc emission factor, EFL_{ij} (grams/mile), is a function of both vehicle weight ($Arcweight_{ij}$) and arc speed(V_{ij}), where $\mathrm{Arcweight}_{ij} = \mathrm{GrossVehicleWeight} - \sum_{\mathrm{p}} \mathrm{D}_{\mathrm{p}}$, and p are the nodes which have been visited before enter arc ij, and D_p is the demand at node p. GrossVehicleWeight is the total vehicle weight at the start of the vehicle journey.

- Node idling emissions, EFN_i (grams/hr), is a function of the average vehicle weight at node j (Nodeweight$_i$), where $\text{Nodewight}_j = \text{Arcweight}_{ij} - 0.5 * D_j$.

5.1.3 Parameter Estimation

To obtain realistic values of commercial vehicle weight/payload and speed in urban areas, we use Texas Commercial Vehicle Surveys data (Nepal et al. 2007) to generate the inputs to the MOVES model summarized in Table 9. The surveys were conducted in several counties in Texas including San Antonio, Amarillo, Valley, Lubbock and Austin during 2005 and 2006 through a vehicle information form and a daily travel log completed by the drivers or operators on an assigned day. The data set includes the trip information such as departure load factor, departure time, arrival time, location, cargo type, cargo drop-off/ pick-up weight; and the vehicle information such as vehicle type, fuel type, gross weight, and odometer readings, etc. More detailed data descriptions are provided in (Ruan et al. 2011). This data set provides the real-world information to estimate the ranges of vehicle weight and dwell time, as well as common commercial vehicle type (single-unit truck) and commercial vehicle travel speeds on arterial streets. Two key parameters, vehicle weight and dwell time, are described in detailed next.

Table 9 Key Input Parameters to MOVES

Input	**Description**
Analysis year	2013
Road type	Urban Unrestricted Access (arterials)
Pollutants	$PM_{2.5}$, Energy consumption
Emission Processes	Running exhaust, crankcase running exhaust, brake and tire wear and tear
Vehicle type	Single Unit Short-haul Truck
Vehicle speed	2.5-75 mph
Vehicle weight (source mass)	4,000-50,000 lbs
Fuel type	Diesel

Error! Reference source not found.GVW and payload

To estimate the emission factors as a function of vehicle weight in MOVES, it is necessary to know the vehicle curb weight and payload. *Vehicle curb weight* is the total weight of a vehicle with standard equipment, all necessary operating consumables, a fuel tank of fuel, while not loaded with cargo. Gross Vehicle Weight (GVW) is the maximum vehicle operating weight specified by the manufacturer, including cargo weight. In other words, a fully loaded vehicle has the following GVW:

$$\text{GVW}=\text{curb weight} + \text{maximum payload} \quad (33)$$

According to the Texas survey data, the range of GVW is between 4,000lbs and 50,000lbs and the ratio of maximum payload to curb weight is between 0.3 and 10 for a single-unit truck with 95% confidence of interval.

Dwell time

Dwell time by cargo type was estimated using a linear regression model with the Texas survey data. It was found that the dwell time was highly correlated with cargo drop-off/pick-up weight at the stop:

For food &beauty products,

$$\text{dwell time (hr)}=0.203*\text{cargo weight } (\times 10^3\text{lbs})+0.192667, \text{ with } R^2=0.53 \quad (34)$$

For farm products,

$$\text{dwell time (hr)}=0.01*\text{cargo weight } (\times 10^3\text{lbs})+0.527017 \text{ with } R^2=0.38 \quad (35)$$

For manufacture equipment products,

$$\text{dwell time (hr)}=0.103*\text{cargo weight } (\times 10^3\text{lbs})+0.582283 \text{ with } R^2=0.42 \quad (36)$$

For parcel products,

$$\text{dwell time (hr)}=0.36*\text{cargo weight } (\times 10^3\text{lbs})+0.121537 \text{ with } R^2=0.37 \quad (37)$$

The numerical results to be shown in Section 3 are based on the dwell time estimates using Eq.34. A sensitivity analysis of cargo type on emissions and energy consumption is presented later in Section 5.3.3.

Finally, after all the parameters were estimated and entered into MOVES, $PM_{2.5}$ emission factors and energy consumption rates are displayed in Figure 10 and Figure 11 for the arcs and nodes respectively.

It is found that the arc energy consumption rates and $PM_{2.5}$ emission factors are decreasing functions of vehicle speed till about 65 mph. On the other hand, they are decreasing at first and then increasing with respect to GVW. For example, the energy consumption rate reaches the lowest around 4,000 lbs of GVW at speed of 25mph and 8,000 lbs at higher speed >30mph. The $PM_{2.5}$ emission factor reaches its minimum point at the GVW of 4,000lbs with a speed<20mph and at 8,000lbs with a speed >25mph. These findings indicate that the optimal route for energy consumption might not be optimal for $PM_{2.5}$ emissions.

The node idling energy consumption rates and $PM_{2.5}$ emission factors are convex functions of GVW; the minimum values occur at the GVW of 20,000lbs and 8,000lbs for energy consumption rate and $PM_{2.5}$ emission factor, respectively. Note that the idling emissions and energy consumption are orders of magnitude lower than those of arcs – for example, for a 8,000lbs truck, $PM_{2.5}$ emissions for an hour dwell time is 0.016 grams while the on-road $PM_{2.5}$ emissions is 10.3grams for an hour at a speed of 20mph. However, idling emissions and energy consumption may add up to an un-negligible amount especially in a congested urban area where customer density is high with large drop-off/ pick-up cargo weights and power-on (idling) is required, e.g., for perishable grocery items.

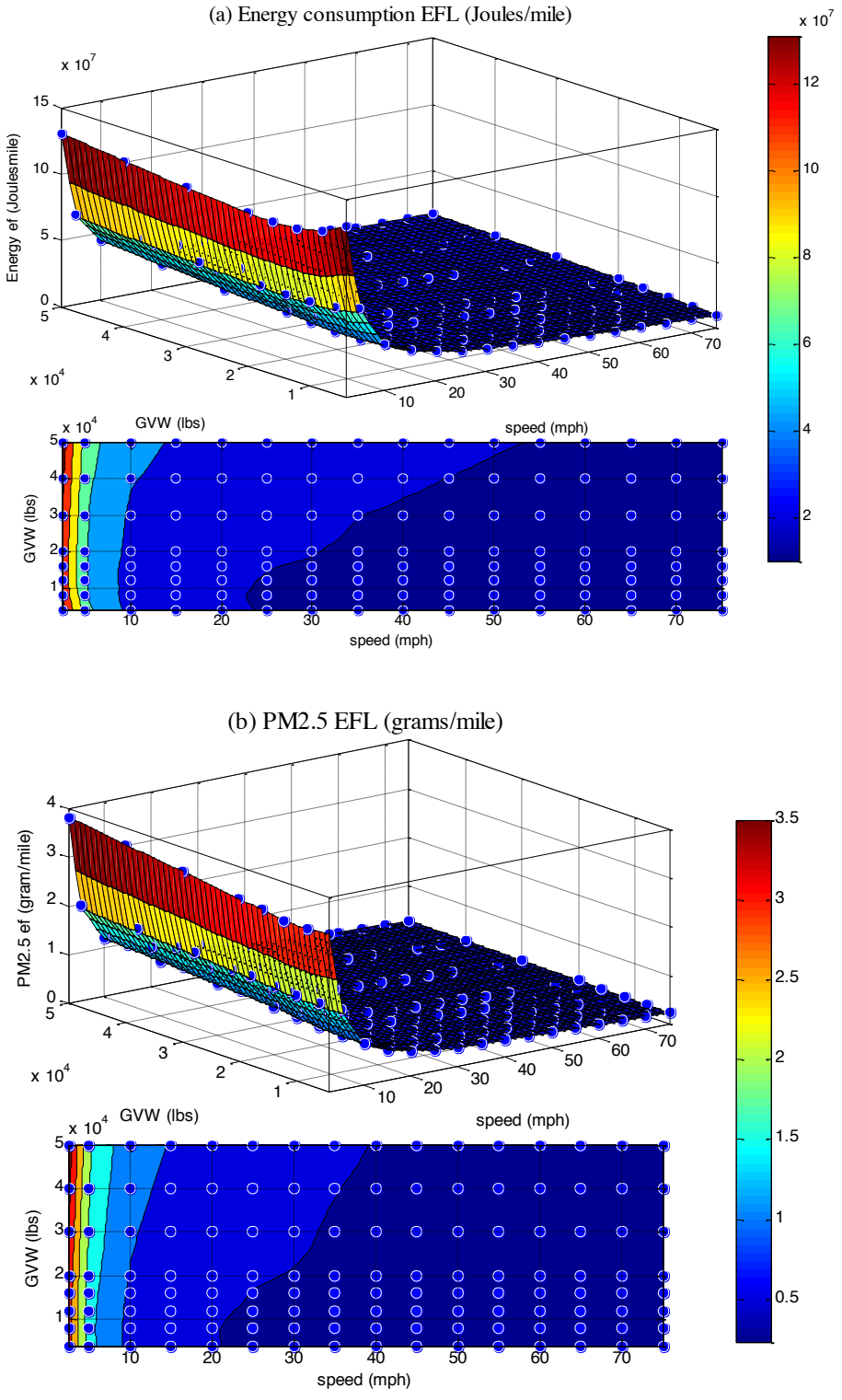

Figure 10 Arc Energy Consumptions (Joules/mile) and PM2.5 Emission Factors (grams/mile) as a Function of GVW and Speed

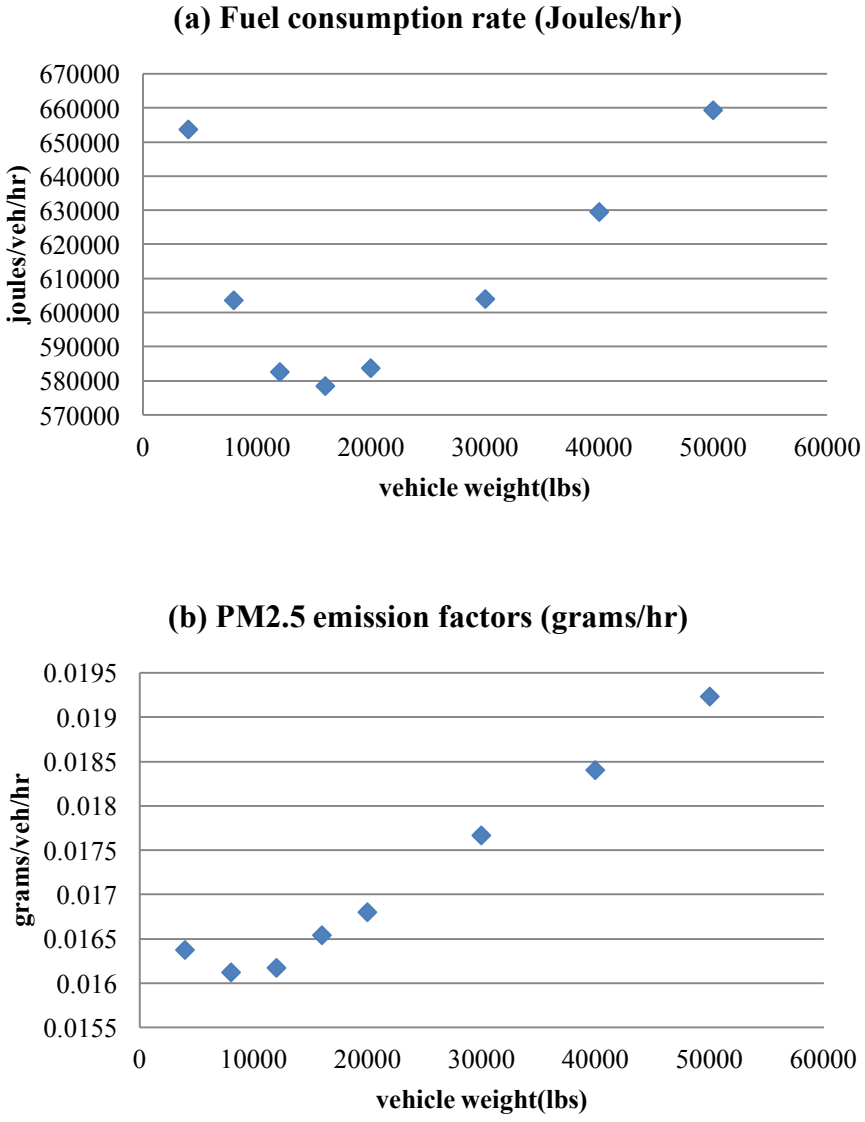

Figure 11 Node Idling Energy Consumptions (Joules/hr) and PM2.5 Emission Factors (grams/hr) as a Function of Vehicle Weight and

5.2 Numerical Example Results

Three different visiting orders were considered in the numerical example defined in Table 8: (A) depot (0)->1->3->2->0, (B) 0->2->3->1->0 , and (C) 0->1->2->3->0. Route B is a reverse order of Route A, and C represents a third alternative routing strategy. Table 10 summarizes the resulting travel distance, energy consumption and $PM_{2.5}$ emissions for the three routing strategies, A, B and C.

Among all the possible routes, it is easy to see that the shortest-path visiting order should be 0-1-3-2-0(Route A), or 0-2-3-1-0 (Route B), and the total distance is 26.03 miles. However, Route B

saves 1.54% of energy consumption and 1.43% of $PM_{2.5}$ emissions from Route A. If the objective is to minimize the energy consumption, then the optimal visiting order should be 0-1-2-3-0 (Route C), with an optimal energy consumption of $5.07x10^8$ joules. Coincidentally, Route C also represents the minimal $PM_{2.5}$ emission routing strategy of 11.87 grams. What is interesting here is that Route C has a 4.5% longer travel distance and yet it brings 5.2% of energy savings and 6.6% less $PM_{2.5}$ emissions compared to Route A. This can be explained by the different vehicle weight distribution during the route in A, B, and C.

Table 10 Numerical Example Results

Route	(i,j)	Arc distance (miles)	Total route distance (miles)	Energy consumption ($\times 10^8$Joules)	$PM_{2.5}$ (grams)
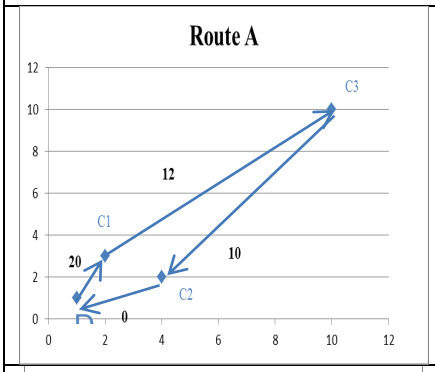	(0,1) (1,3) (3,2) (2,0)	2.2 10.6 10.0 3.2	**26.03**	Arcs:5.32 Nodes:0.0296 Total:5.35	Arcs:12.62 Nodes:0.0846 Total:12.70
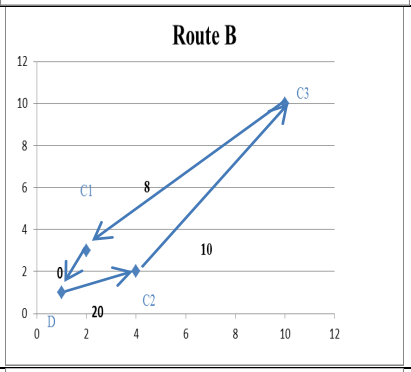	(0,2) (2,3) (3,1) (1,0)	3.2 10.0 10.6 2.2	**26.03**	Arcs:5.24 Nodes:0.0297 Total:5.27	Arcs:12.44 Nodes:0.0845 Total:12.52
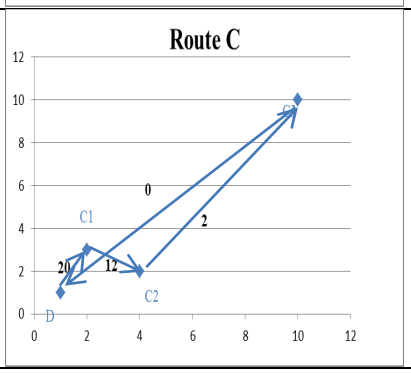	(0,1) (1,2) (2,3) (3,0)	2.2 2.2 10.0 12.7	**27.2**	Arcs:5.04 Nodes:0.0297 Total:5.07	Arcs:11.79 Nodes:0.0847 Total:11.87

In Route C, the customer with the smallest demand (C3) is served last, which means the heavier goods are unloaded first and early so the vehicle is traveling lighter for the most part of the route than in Route A or B. Thus the arc emissions and energy consumption are lowered more than in Routes A and B – recall the increasing effect of GVW on emissions and energy consumption (at speed of 30 mph) shown in Figure 10. Note that Route C has slightly higher idling emissions because serving larger demand customers first while GVW is higher increases the idling emissions slightly than that with a lower GVW. Overall from a sustainable routing stand point of view, Route C represents the most economical (in terms of energy consumption) and environmental friendly (in terms of $PM_{2.5}$ emissions) routing strategy. The flip side is that Route C incurs longer travel distance (or time). In reality, if there is a time window constraint, the energy savings and environmental benefits may be dampened and even become negative.

5.3. Sensitivity Analyses

The numeric example results have demonstrated that considering vehicle weight and speed in routing can bring savings on energy consumption and/or $PM_{2.5}$ emissions. This section examines to what extent different factors may contribute to the savings by a serials of sensitivity analyses defined in Table 11. Using Route A as a base, each analysis calculates the percent changes of distance, energy consumption and $PM_{2.5}$ for Routes B and C, respectively, from Route A. A positive value indicates that route A is preferable and a negative value demonstrates Route B or Route C brings savings.

Table 11 Summary of the Scenarios in Sensitivity Analysis

Factors	**Test value**	**Section**
GVW(lbs) Weight ratio(payload/curb weight)	8k, 16k, 30k, 45k 0.5, 1, 2.75, 5	5.3.1
Constant speed across arcs (mph)	5, 10, 20, 30, 40, 55, 70	5.3.2
Variant speed across arcs (mph)	Various speed profiles representing various traffic conditions	5.3.2
Cargo type(or dwell time) GVW (lbs)	Farm, manufacturing, food, parcel 16k, 30k, 45k	5.3.3

5.3.1 Effect of GVW and Weight Ratio

This section tests the percentage changes of energy consumption and $PM_{2.5}$ emissions for Routes B and C, respectively, from Route A by GVW and weight ratio (defined as payload/curb weight). For the same GVW, a larger weight ratio means a larger payload.

Table 12 and Table 13 summarize the percentage changes. As expected, Route C generally has higher energy and emissions savings from Route A than Route B. For a given weight ratio, more savings are resulted for heavier GVW for both B and C. For GVW greater than 16,000 lbs, larger weight ratios render more energy and emissions savings on both B and C; less than 16,000 lbs,

both B and C actually have worse energy and emissions performance than A. Such a pattern can be explained by the similar pattern in the idling energy consumption and emissions shown in Figure 11. In general, heavier vehicles with larger initial payloads can benefit more from the sustainable routing strategies which incorporate the effect of vehicle weight.

Table 12 Effect of GVW and Weight Ratio: Percentage Change from Route A to B

Percentage change (B-A)%	GVW (lbs)/ Weight ratio	8,000	16,000	30,000	45,000
Energy consumption	0.5	0.17%	-0.39%	-0.54%	-0.84%
	1	0.25%	-0.30%	-0.81%	-1.35%
	2.75		-0.19%	-1.60%	-1.74%
	5			-2.10%	-2.03%
$PM_{2.5}$	0.5	0.02%	-0.51%	-0.51%	-0.75%
	1	0.04%	-0.52%	-0.71%	-1.16%
	2.75		-0.49%	-1.61%	-1.53%
	5			-2.29%	-1.80%

Table 13 Effect of GVW and Weight Ratio: Percentage Change from Route A to C

Percentage change (C-A)%	GVW (lbs)/ Weight ratio	8,000	16,000	30,000	45,000
Energy consumption	0.5	5.83%	2.68%	0.14%	-2.12%
	1	6.48%	3.41%	-2.64%	-4.95%
	2.75		7.10%	-3.90%	-9.67%
	5			-1.25%	-9.69%
$PM_{2.5}$	0.5	4.69%	1.55%	0.41%	-1.25%
	1	4.78%	1.52%	-3.00%	-4.09%
	2.75		3.06%	-6.85%	-10.26%
	5			-6.05%	-12.10%

5.3.2 Effect of Speed

(I) Constant Speed Across Arcs

In this section, vehicle speed is assumed constant across all arcs in the graph and its value varies from 5mph to 70 mph. The percentage changes (B from A and C from A respectively) are shown in Figure 12. The trends are similar in both cases. That is, increasing energy consumption savings are gained when speed goes up from 5 mph till around 20 to 30 mph; then the savings drop slightly until around 40mph and go up again afterwards. This seems to indicate that, road traffic being equally good or bad, more energy savings can be expected on congested urban roadways as well as on highways with the new sustainable routing strategies. $PM_{2.5}$ emissions savings display the similar trend to that of energy consumption at lower speed (between 5 and 30mph) but then

continuously decrease at higher speeds. These findings suggest that the optimal routing speeds for minimizing $PM_{2.5}$ emissions and energy consumption may be different.

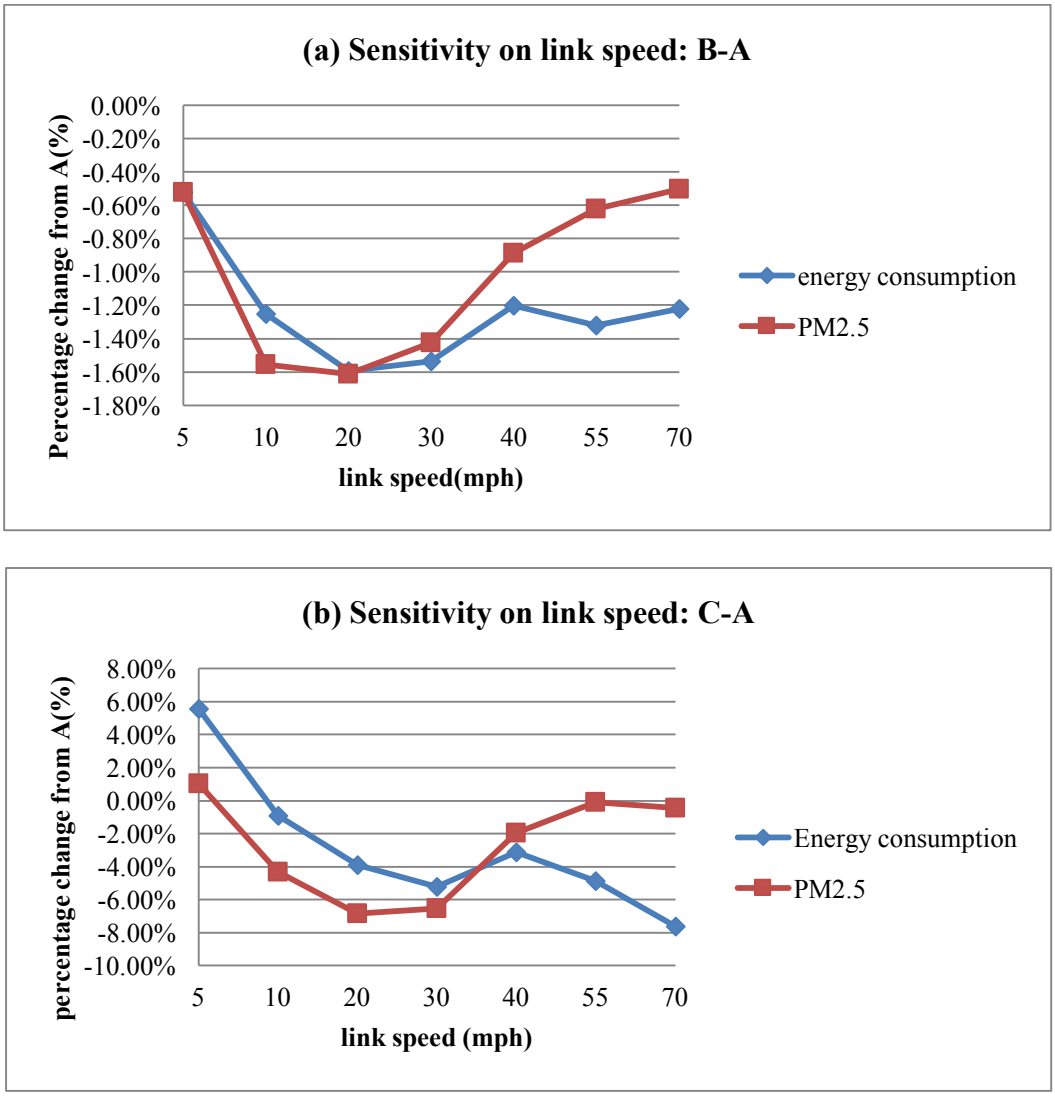

Figure 12 Sensitivity on Speed Bin

(II) Variant Speed Across Arcs

Table 14 defines three speed profiles where different traffic conditions (congested versus uncongested, highways versus urban arterials) could be encountered during the vehicle's journey. Table 15 summarizes the percentage change results between Routes B and A and Routes C and A.

In Profile 1, Routes A and B have the exact same arc speeds but in the reverse directions - recall that Route B is in the reverse visiting order of Route A; and Route C has a very low speed arc (3,0), which has the longest travel distance than any other arcs in Route A, B, or C. As a result, Route C actually has higher energy consumption and $PM_{2.5}$ emissions compared to Route A.

In Profile 2, three of the four arcs in Route A have very low speeds (congested); Route B has considerably much higher speeds (highway speeds) than those in Route A and the heaviest arc in Route B (0,2) has the highest speed among all arcs; Route C also has better speed performance than Route A albeit not as high speeds as Route B. What we see now is that both Routes B and C display significant savings in energy and $PM_{2.5}$ emissions over Route A.

In Profile 3, now Route A has much higher speeds than Route B and arc speeds on Route C are comparable to those on Route A. As a result, Route B has the worst energy and emissions performance among the three routes and Route C also has higher energy consumption and emissions than Route A likely due to the low speed on the longest arc (3,0).

To summarize, the one thing that is clear in this analysis is that speed greatly impacts energy consumption and emissions and low speeds seem to have the greater impact, causing higher energy consumption and emissions.

Table 14 Variant Speed Profiles

Route	link	Speed profile (mph)		
		Profile 1	Profile 2	Profile 3
A	(0,1)	32	3	73
A	(1,3)	14	5	49
A	(3,2)	68	39	60
A	(2,0)	73	7	34
B	(0,2)	73	61	32
B	(2,3)	68	61	62
B	(3,1)	14	54	6
B	(1,0)	32	11	10
C	(0,1)	32	3	73
C	(1,2)	33	49	13
C	(2,3)	68	61	62
C	(3,0)	8	39	29

Table 15 Sensitivity of Speed

Speed profile	Percentage change B-A		Percentage change C-A	
	Energy	$PM_{2.5}$	Energy	$PM_{2.5}$
Profile 1	-2.35%	-4.71%	38.63%	43.15%
Profile 2	-65.82%	-71.52%	-50.21%	-53.58%
Profile 3	116.24%	157.49%	16.86%	22.98%

5.3.3 Effect of Cargo Type (or Dwell Time)

As described in section 5.1.3, dwell time is a linear function of the drop-off/ pickup cargo weight at the customer locations for different cargo types. The cargo unit service times ($\times 10^3$lbs/hr), i.e., the coefficients in the linear models Eq. 34-37, vary between from 0.01(farm products) to 0.36 (parcels). Using the cargo unit service time for food and beauty products as the baseline, a term called *cargo service ratio* is introduced to measure the cargo unit service time ratio between a specified type of cargo and the baseline cargo type. Cargo service ratio reflects the relative loading/unloading speed, which is affected by the cargo characteristics such as packaging method and value-to-weight ratio. As such, farm products have a cargo service ratio of 0.05, manufactured goods 0.51, and parcels 1.77. In other words, parcels have the longest unit service time among the four cargo types considered and farm products have the least unit service time.

Table 16 shows the following results for Route C: percent idling emissions of the total $PM_{2.5}$ emissions, and the percentage changes of energy consumption and $PM_{2.5}$ emissions from route A. By varying the GVW from 16000 to 45000 lbs while keeping the weight ratio (Payload-to-curb-weight ratio) constant at 2.75, it represents the different demand levels are served.

As expected, the higher the cargo service time the higher the idling emissions in percentage share. Both the energy and $PM_{2.5}$ emissions savings on Route C go down very slightly from farm products to parcels in an ascending order of cargo service ratio. But overall because both the idling emissions and energy consumptions account for a very small portion of the total quantities as already discussed earlier, the effect of cargo type (or dwell time) is very small (to the second decimal point in the percentage changes).

Table 16 Effect of Cargo Type

Cargo type	GVW	Weight ratio	Cargo service ratio	% node idling emissions		percentage change from A: C-A	
				Energy	$PM_{2.5}$	energy	$PM_{2.5}$
Farm	16000	2.75	0.05	0.17%	0.19%	7.11%	3.07%
Farm	30000	2.75	0.05	0.18%	0.20%	-3.92%	-6.88%
Farm	45000	2.75	0.05	0.18%	0.21%	-9.72%	-10.32%
Manufactured	16000	2.75	0.51	0.29%	0.34%	7.10%	3.06%
Manufactured	30000	2.75	0.51	0.39%	0.45%	-3.91%	-6.86%
Manufactured	45000	2.75	0.51	0.49%	0.56%	-9.69%	-10.29%
Food	16000	2.75	1	0.29%	0.34%	7.10%	3.06%
Food	30000	2.75	1	0.49%	0.57%	-3.92%	-6.85%
Food	45000	2.75	1	0.69%	0.80%	-9.67%	-10.26%
Parcels	16000	2.75	1.77	0.45%	0.52%	7.09%	3.06%
Parcels	30000	2.75	1.77	0.80%	0.94%	-3.89%	-6.83%
Parcels	45000	2.75	1.77	1.15%	1.34%	-9.63%	-10.21%

5.4 Conclusions

Using a numerical example, this study has demonstrated the noticeable (joint) effects of vehicle payload, vehicle speed, and dwell time on urban commercial vehicle emissions and energy consumption. For example, heavier vehicles with larger initial payloads can benefit more from the sustainable routing strategies which incorporate the effect of vehicle weight, and low speeds have the greater impact than high speeds, causing higher energy consumption and emissions. The analysis results have indicated that the vehicle payload and speed could affect the visiting order of a distribution tour if minimizing the energy consumption or emissions is the objective. Idling energy consumption/emissions at stops, although considerably low compared to on-road energy consumption/emissions, may not be ignored especially in congested urban areas where customer density is high with large drop-off/ pick-up cargo weights and other special requirements are in place at the customer's (e.g., engine on to operate the refrigerator).

As an ongoing research effort, this research team is currently working on the formulation of a new kind of sustainable CVRP problem which considers energy consumption /emissions as a function of, in addition to vehicle speed, vehicle weight (or payload) on links/arcs and nodes as well as vehicle dwell time. In future research, other variations such as time window constraint and loading activities at the customers during the same route (which is also related to the capacity constraint) need to be incorporated. It is also necessary to test the new routing algorithms on selected real-world goods distribution cases based on real-world data.

6. REFERENCES

Ahn, K. and Rakha, H.(2008). The effects of route choice decisions on vehicle energy consumption and emissions. *Transportation Research Part D*, 13:151–167.

Arvidsson, N. (2013). The milk run revisited: A load factor paradox with economic and environmental implications for urban freight transport. *Transportation Research Part A: Policy and Practice*, *51*, 56-62.

Barth, M., An, F., Norbeck, J. and Ross, M.(1996). Modal emissions modeling: a physical approach. *Journal of the Transportation Research Board*, 1520:81–88.

Barth, M., An, F., Younglove, T., Scora, G., Levine, C., Ross, M. and Wenzel, T. (2000). Development of a comprehensive modal emissions model. Technical report, National Cooperative Highway Research Program.

Bauer, J., Bektas, T. and Crainic, T.G. (2009). Minimizing greenhouse gas emissions in intermodal freight transport: an application to rail service design. *Journal of the Operational Research Society*, 61(3):530–542.

Bawa, V. S. (1975). Optimal rules for ordering uncertian prospects. *Financial Economics*, 2:95–121.

Bektas, T. and Laporte, G. (2011). The pollution-routing problem. *Transportation Research Part B*, 45:1232–1250.

Benedek, C.M. and Rilett, L.R. (1998). Equitable traffic assignment with environmental cost functions. *Journal of transportation engineering*, 124(1):16–22.

Bishins, A., Winkelman, S. and Kooshian, C. (2009). Cost-effective GHG reductions through smart growth & improved transportation choice. Technical report.

Boriboonsomsin, K., Vu, A. and Barth, M. (2010). Eco-driving: Pilot evaluation of driving behavior changes among us drivers. Technical report.

Cambridge Systematics (2009), *Moving Cooler*, Urban Land Institute.

Chen, A., Zhou, Z. and Ryu, S.(2011). Modeling physical and environmental side constraints in traffic equilibrium problem. *International Journal of Sustainable Transportation*, 5:3:172–197.

Consulting, I. C. F. (2005). Assessing the effects of freight movement on air quality at the national and regional level. *April, Washington, DC: US Department of Transportation*.

Davies, J. and Facanha, C. (2007) Greenhouse gas emissions from freight trucks, presented at *the 16th Annual International Emission Inventory Conference: Emission Inventories: "Integration, Analysis, and Communications",* Raleigh, May 14-17, 2007

Dentcheva, D. and Ruszczynski, A. (2003). Optimization with stochastic dominance constraints. *SIAM Journal of Optimization*, 14(2):548–566.

Farradyne, P. B.(2000), *Traffic Incident Management Handbook*, Federal Highway Administration.

Eguia, I., Racero, J., Molina, J. C., & Guerrero, F. (2013). Environmental Issues in Vehicle Routing Problems. In *Sustainability Appraisal: Quantitative Methods and Mathematical Techniques for Environmental Performance Evaluation* (pp. 215-241). Springer Berlin Heidelberg.

Farrington, R. and Rugh, J. (2000). Impact of vehicle air-conditioning on fuel economy, tailpipe emissions, and electric vehicle range. In *Earth Technologies Forum, WDC*.

Figliozzi, M. (2010). Vehicle routing problem for emissions minimization. *Transportation Research Record: Journal of the Transportation Research Board*, *2197*(1), 1-7.

Friedman, M. and Savage, L.P.(1948). The utility analysis of choices involving risk. *Journal of Political Economy*, 56:279–304.

Frey, H. C., Unal, A., Rouphail, N. M. and Colyar, J. D. (2003), 'On-road measurement of vehicle tailpipe emissions using a portable instrument', *Journal of the Air & Waste Management Association* 53(8), 992-1002.

Gaines, L., Vyas, A., & Anderson, J. L. (2006). Estimation of fuel use by idling commercial trucks. *Transportation Research Record: Journal of the Transportation Research Board*, *1983*(1), 91-98.

Hadar, J. and Russell, W. R. (1971). Stochastic dominance and diversification. *Journal of Economic Theory*, 3:288–305.

Hanoch, G. and Levy, H.(1969). The efficiency analysis of choices involving risk. *Review of Economics studies*, 36:335–346.

Kara, I., Kara, B. and Yetis, M. (2007). Energy minimizing vehicle routing problem. *Combinatorial Optimization and Applications*, 4616:62–71.

Kirby, R.F. and Potts, R.B. (1969). The minimum route problem for networks with turn penalties and prohibitions. *Transportation Research*, 3(3):397–408.

Maden, W., Eglese, R. and Black, D. (2009). Vehicle routing and scheduling with time-varying data: A case study. *Journal of the Operational Research Society*, 61(3):515–522.

Mannering, F.L., Kilareski, W.P. and Washburn, S.S. (2005). *Principles of Highway Engineering and Traffic Analysis*. John Wiley & Sons Inc.

Manzie, C., Watson, H., and Halgamuge, S. (2007). Fuel economy improvements for urban driving: Hybrid vs. intelligent vehicles. *Transportation Research Part C*, 15(1):1–16.

mpgforspeed.com: http://www.mpgforspeed.com/, last accessed May 2014.

Nagurney, A.(2000). Congested urban transportation networks and emission paradoxes. *Transportation Re- search Part D*, 5:145–151.

Nam, E.K. (2003) Proof of concept investigation for the physical emission rate estimator (PERE) for MOVES. Technical Report 420.

Nepal, S.A., Farnsworth, S.P. and Pearson, D.F. (2007). *2006 San Antonio Area Commercial Vehicle Survey Technical Summary.* Texas Transportation Institute.

Nie, Y., Wu, X. and Homem de Mello, T. (2011). Optimal path problems with second-order stochastic dominance constraints. *Networks and Spatial Economics*, Vol. 12, No. 4, pp. 561-587.

Nie, Y. and Li, Q. (2012). An eco-routing model considering microscopic vehicle operating conditions. *Working paper*, Northwestern Univerity.

Onoda, T. (2009), 'Iea policies g8 recommendations and an afterwards', *Energy Policy* **37**(10), 3823–3831.

Penic, M.A. and Upchurch, J.(1992). Transyt-7f, enhancement for fuel consumption, pollution emissions, and user costs. *Journal of Transportation Research Board*, 1360

Rilett, L.R. and Benedek, C.M. (1994). Traffic assignment under environmental and equity objectives. *Transportation Research record*, 1443:92–99.

Ruan, M., J. Lin, K. Kawamura (2011) *Modeling Commercial Vehicle Daily Tour Chaining, the 90th Transportation Research Board Annual Meeting*, National Research Council, Washington, D.C., 2011

Sugawara, S. and Niemeier, D.A.(2002). How much can vehicle emissions be reduced? exploratory analysis of an upper boundary using an emissions-optimized trip assignment. *Journal of Transportation Research Board*, 2260:29–37.

Suzuki, Y. (2011). A new truck-routing approach for reducing fuel consumption and pollutants emission. *Transportation Research Part D: Transport and Environment*, *16*(1), 73-77.

The truckers report, available at http://www.thetruckersreport.com/infographics/cost-of-trucking/. last accessed in July 2013.

Tzeng, G.H. and Chen, C.H (1993). Multi-objective decision making for traffic assignment. *IEEE Transactions on engineering management*, 40:180–187.

Toth, P., & Vigo, D. (Eds.). (2002). *The vehicle routing problem* (Vol. 9). Siam.

US Environmental Protection Agency (2002). User guide to mobile 6.1 and 6.2. Technical report, Office of Transportation and Air Quality.

US Environmental Protection Agency(EPA)(2010), "*Motor Vehicle Emission Simulator. MOVES 2010b User Guide,*" Office of Transportation and Air Quality.

Wu, X. and Nie, Y. (2011). Modeling heterogeneous risk-taking behavior in route choice: A stochastic dominance approach. *Transportation Research Part A*, Vol. 45, No. 9, pp. 896-915

Wygonik, E., & Goodchild, A. (2011). Using a GIS-based emissions minimization vehicle routing problem with time windows (EVRPTW) model to evaluate CO_2 emissions and cost trade-offs in a case study of an urban delivery system. In *Transportation Research Board 90th Annual Meeting* (No. 11-1109).

Xiao, Y., Zhao, Q., Kaku, I., & Xu, Y. (2012). Development of a fuel consumption optimization model for the capacitated vehicle routing problem. *Computers & Operations Research*, *39*(7), 1419-1431.

Yin, Y. and Lawphongpanich, S.(1998). Internalizing emission externality on road networks. *Computers and Operations Research*, 25(6):457–468

Yin, Y. and Lawphongpanich, S. (2006). Internalizing emission externality on road networks. *Transportation Research Part D*, 11(4):292–301.

Ziliaskopoulos, A.K. and Mahmassani, H.S. (1996). A note on least time path computation considering delays and prohibitions for intersection movements. *Transportation Research Part B*, 30(5):359–367.

CFIRE

University of Wisconsin-Madison
Department of Civil and Environmental Engineering
1410 Engineering Drive, Room 270
Madison, WI 53706
Phone: 608-263-3175
Fax: 608-263-2512
cfire.wistrans.org